2016

Effective Lengths of Web Members in Trusses - an Experimental Investigation of Tension Effects

Allison Louise Partridge
Bucknell University, alp020@bucknell.edu

EFFECTIVE LENGTHS OF WEB MEMBERS IN TRUSSES – AN EXPERIMENTAL INVESTIGATION OF TENSION EFFECTS

by

Allison L. Partridge

A Thesis Submitted to the Honors Council

For Honors in Civil Engineering

at Bucknell University

May 2016

Approved by:

Adviser: Ronald Ziemian. Professor of Civil Engineering

Adviser: Jean Batista Abreu, Visiting Professor of Civil Engineering

Department Chairperson: Michael Malusis, Associate Professor of Civil Engineering

ACKNOWLEDGEMENTS

I would like to thank my advisors, Professors Ron Ziemian and Jean Batista, for giving me the opportunity to pursue this research and for constantly providing guidance and support throughout the past two semesters. Additionally, to Professor Salyards and Professor Buonopane, for listening when I questioned aspects of my work, and providing much needed suggestions and continuous support.

I cannot thank Jim Gutelius enough for all of his help in taking my designs and bringing them to life and for the countless times I questioned whether it was ever going to work.

I would also like to thank my family for always encouraging me and keeping me motivated when I questioned the path I was taking. Lastly, I cannot thank my friends enough for providing distractions when desperately needed, and the encouragement and support that without I couldn't have survived the last two semesters, let alone the past four years.

TABLE OF CONTENTS

LIST OF TABLES

LIST OF FIGURES

ABSTRACT

Throughout the truss and joist industry, research is constantly underway in an effort to determine ways to further minimize production costs and material use. In regard to structural stability, previous research has shown that the effective length factor, *K*, for web members may be overly conservative, leading to an overuse of material in the design. Currently, the top and bottom chords provide the only acknowledged flexural and torsional resistance for compression web members in trusses. This study presents an investigation into the restraining effects provided by tension members in trusses, which is in an effort to determine whether the tensioning effect is adequate to warrant the use of a smaller *K*-factor in routine design.

Two different methods to explore the buckling mode of compression web members are performed for this research, including (1) the use of an experimental testing apparatus, and (2) computational analysis of compression web members within a modified Pratt truss. The results are presented and summarized based on the nature of the research method. Results of the experimental testing confirmed the presence of additional rotational restraint provided by tension members. Therefore, it was concluded that effective length factors for compression web members need not exceed a value of 1.0. The computational studies of a modified Pratt truss supported this conclusion and further suggest that a *K*-factor of less than 1.0 could be used in design, provided that sufficient resistance to out-of-plane translation is present along the bottom chord (via bracing or

other means). Recommendations for future work, including full-scale testing and additional computational studies, are provided within this thesis.

CHAPTER 1: INTRODUCTION AND LITERATURE REVIEW

1.1 Thesis Statement

An experimental model and associated computational studies will show that the design of compression web members in trusses should account for the stabilizing effects of the neighboring tension members when calculating the effective buckling lengths for which they are designed.

1.2 Introduction

A truss is a structural system often used in buildings to provide for long, clear-spans when large open areas are required. Trusses are often used in place of beams, as they have been proven to be more economical for use in long-span building design. Trusses are comprised of two main structural components, including web members and chords. Web members connect the top and bottom members (chords) of the truss, which, depending on the configuration and load conditions, may act in tension or compression (see example in Figure 1.1).

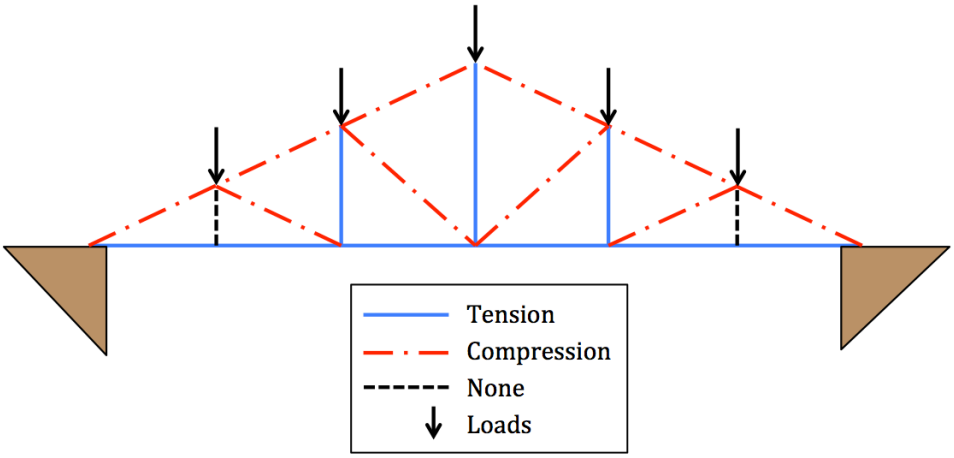

Figure 1.1. Typical Truss System with Members Labeled for Tension and Compression

Currently, organizations, such as the Steel Joist Institute or the American Iron and Steel Institute, provide the governing design guidelines for compression web members through the application of the Effective Length Method (further explained in Section 1.5.1). Given that the focus of this thesis is on compression web members in trusses, it is assumed that there is no intentional bending moment at or between the ends of the members, thereby making it possible to refer to the idealized pinned connection conditions present at the end of members. This assumption also allows for the application of Equation (1.1) to calculate the flexural buckling strength, P_{cr}, of a compression member,

$$P_{cr} = \frac{\pi^2 EI}{(KL)^2} \tag{1.1}$$

where E is the elastic modulus of the material, I is the moment of inertia of the cross section, L is the unbraced length of the member, and K is the effective length factor,

which accounts for the degree of rotational and translational restraint provided at the member ends (Lee, 2013).

The flexural buckling strength of columns is often determined through computer analysis. From this analysis, a critical buckling load, P_{cr}, is determined and can be used to back-calculate the effective length factor, K, by rewriting Equation (1.1) into the following form to solve for K:

$$K = \frac{\pi}{L}\sqrt{\frac{EI}{P_{cr}}} \tag{1.2}$$

This thesis will focus on evaluating the accuracy of the effective length factors currently specified in the design procedures for out-of-plane buckling of compression web members.

1.3 Purpose and Objectives

The use of trusses and joists in building design has increased over the past twenty years as their production costs have significantly decreased, allowing for more flexibility in design. As a result, additional research is underway in an effort to determine ways to further minimize production costs and material use. One focus area has been on examining the design procedures used for chord and web members. In particular, research has shown that the effective length factor, K, for web members may be overly conservative, leading to an overuse of material in their design (Lee, 2013).

For compression web members in trusses, the top and bottom chords provide the only acknowledged flexural and torsional resistance. Research performed on open-web steel joists, however, suggests that the adjacent tension web members may provide additional out-of-plane flexural stiffness that could be accounted for in the calculation of a reduced effective length factor, which is known to be inversely proportional to the compressive strength (Lee & Ziemian, 2014). The additional flexural end restraint provided by these tension members suggests that the current *K*-factor used for design is conservative, and a decreased factor would maintain the safety of structures while increasing efficiency. The primary objective of this thesis is to construct an experimental testing apparatus to physically model and examine the effects of tension members on the buckling mode and corresponding buckling strength of compression web members. Additionally, computational studies will be performed to determine how well the observed restraining effects would apply on a full-size truss.

The primary objectives of this experimental and analytical research include the following:

- Understand out-of-plane flexural buckling behavior of compression web members
- Determine whether neighboring tension members provide any significant out-of-plane restraint
- Determine if out-of-plane K-factors less than 1.0 can be used to design compression web members
- Explore the previous objectives based on the following two considerations:

- Inverted King Post Truss: experimental model
- Modified Pratt Truss (cold-formed roof truss): computational studies

1.4 Research Method

The primary methods of research for this thesis involve the construction of an experimental testing apparatus in conjunction with computational results from computer analysis studies. Supporting differential equations will be analyzed to corroborate the experimental theory and collected results. The small-scale experimental testing program is designed to investigate the effects of neighboring tension members on out-of-plane buckling of compression web members. To determine whether the same tensioning effects occur within a system of members, these results will then be applied to a larger scale through the truss analysis studies. In order to perform the truss analysis, out-of-plane *K*-factors will be determined through an equivalent column method developed throughout the course of this research. This method utilizes induced compressive strains to buckle the member of interest by means of the self-equilibrating induced-compression (SEIC) method (Lee, 2013). All computational analyses will be performed using the finite element analysis program, MASTAN2, developed by Ziemian and McGuire (2016).

1.5 Background

The *Guide to Design Criteria for Metal Compression Members* establishes the methods to be used for members that are part of a framework, in which there is no intentional bending moment introduced at or between the ends by frame action or intermediate lateral loads (Johnston, 1966). The buckled behavior of such members can be determined primarily through an examination of the restraints imposed by the framework and surrounding members, rather than the entire frame system (Johnston, 1966).

The restraint provided by the framework is categorized into two main restraining forces: flexural restraint, which can prevent rotation about any axis at the end of the member, and translational restraint, which can prevent displacement in any linear direction (Johnston, 1966). End restraints are categorized based on the extent to which they provide flexural and/or translational restraint. Columns are then analyzed based on their end conditions and the associated effective length factor that is determined based on the individual combination of end restraints.

This thesis explores the impacts of varying end restraints to determine a model that would provide a more accurate representation of the behavior of compression web members in truss systems. An important aspect of this research is determining the direction of the resulting buckled force and how that impacts the effective length of the buckled column of interest. This theory was explored first in Lee's research (2013) on open web steel joists. A summary of his results and research methods is provided in Section 1.5.2.

1.5.1 Effective Length Method (ELM)

The Effective Length Method is the current standard used in the design of compression web members in trusses. The effective length, *KL,* of a column is defined as the distance between successive inflection points, or points of zero moment.

In this thesis, the effective length, *KL*, of the members of interest will be determined through the use of the equivalent elastic column-buckling load, Equation (1.1). This method is used, as an alternative to the application of elastic (or inelastic) stability theory, as a way to calculate the compressive strength of a column (AISC, 2010). The equivalent elastic column-buckling method is dependent on the end support conditions of a column and the degree to which they impact the buckled length and thereby the buckling load. The table in Figure 1.2 provides the theoretical effective length factor, *K,* values and those recommended for use in design for the idealized end conditions displayed (AISC, 2010).

TABLE C-A-7.1
Approximate Values of Effective Length Factor, *K*

	(a)	(b)	(c)	(d)	(e)	(f)
Buckled shape of column is shown by dashed line	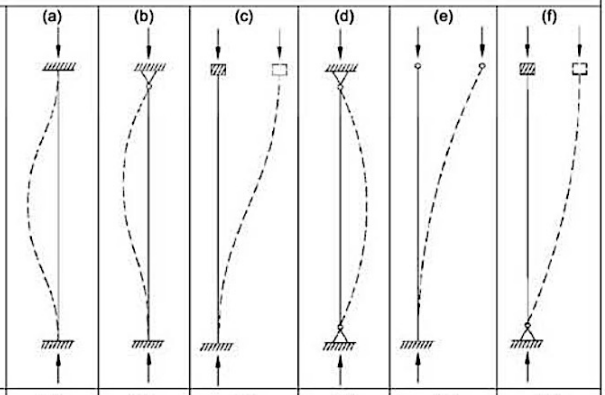					
Theoretical *K* value	0.5	0.7	1.0	1.0	2.0	2.0
Recommended design value when ideal conditions are approximated	0.65	0.80	1.2	1.0	2.1	2.0
End condition code	Rotation fixed and translation fixed Rotation free and translation fixed Rotation fixed and translation free Rotation free and translation free					

Figure 1.2. Effective length factors for various end support conditions (AISC, 2010)

The Steel Joist Institute (SJI, 2010), along with the *Guide to Design Criteria for Metal Compression Members,* specifies a *K*-factor of 1.0 for use in the out-of-plane design of compression web members. This *K*-factor would be accurate under the assumption that the top and bottom chords, along with adjacent tension members, provide no rotational restraint on the compression member as shown in case (d) in Figure 1.2. This thesis will explore the extent to which this assumption is valid within truss systems and whether or not a design value of K<1.0 is overly conservative.

1.5.2 Literature Review

Lee's research (2010) investigated the accuracy of the current effective length factors specified for compression web member design in open-web steel joists. His research focused on two types of steel joists and examined the in-plane and out-of-plane behavior of the compression web members. Lee suggested that the out-of-plane *K*-factor is bound between 0.5 and 1.0 based on the behavior of the restraining force that develops on the compression web member through the interaction with the bottom chord and adjacent tension web members. The simplified model used to demonstrate how the resisting force of the tension cables tracks (remains aligned with) a chord defined by the column ends is shown in Figure 1.3 (a). This is compared with the resisting force in the system in Figure 1.3 (b) always remains vertical.

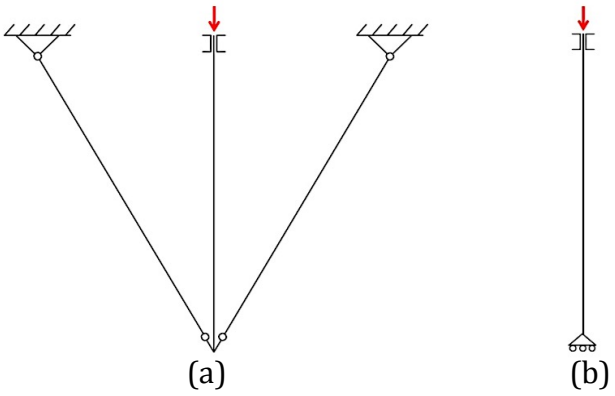

Figure 1.3 (a) & (b). Compression member with (left) and without (right) additional tension cables

The experimental research for this thesis will create physical representations of the two systems shown in Figure 1.3 to further explore and support Lee's claim.

1.6 Construction Assistance

Throughout the experimental portion of this research, Jim Gutelius, the Bucknell structural engineering laboratory director, assisted with the apparatus construction. Once provided with dimensioned designs Jim constructed the preliminary apparatus and assisted in subsequent design alterations throughout the calibration-testing phase. Jim provided invaluable assistance in determining appropriate material selections for the various aspects of the experimental design.

1.7 Thesis Overview

This thesis is organized into five chapters. Chapter 1 provides an introduction to the thesis topic and purpose for the research. Chapter 2 covers all of the experimental and computational studies associated with an inverted king post truss model. This chapter includes all associated methodology and results. Chapter 3 presents all of the methodology and collected results of studies performed on a modified Pratt truss model. Chapter 4 interprets the results from the two analysis methods. Chapter 5 provides the conclusions, and suggestions for additional research that should be done on the subject.

CHAPTER 2: INVERTED KING-POST TRUSS STUDIES

The construction of a scaled experimental model, with geometry reflective of an inverted king-post truss, is the main focus of the experimental testing portion of this research. The typical geometry of an inverted king-post can be seen in Figure 2.1 (Leet et al., 2010). The main structural components include a compressive central post (web member), surrounding tension cable, which behaves similar to a bottom chord, and a beam acting as the top chord.

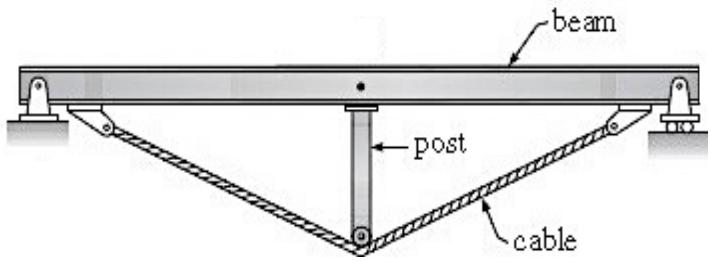

Figure 2.1. Structural components of an inverted king-post truss (Leet et al., 2010)

This configuration provides a simplified model that highlights the member interaction central to this thesis; that of the compressive web member and neighboring tension members. This chapter describes the experimental and computational methodology used throughout the course of this research to analyze and compare the experimental inverted king-post system, along with additional experimental configurations.

2.1 Experimental Testing

The experimental testing portion of this research revolves around the construction and testing of different exploratory configurations to examine the effects of tension members on the buckling mode, and corresponding buckling strength of compression web members. The following sections outline the experimental methodology associated with the testing apparatus, and report the collected results of the experimental testing.

2.1.1 Experimental Methodology

This section describes the methodology behind the experimental testing portion of this research, which is separated into three distinct subsections. The first phase focuses on establishing the preliminary design of the experimental testing apparatus. The second phase includes the complete construction and calibration of the testing apparatus. The final phase encompasses the development and execution of the experimental testing program.

2.1.1.1 Preliminary Design

The designs of the experimental systems are intended to model the effects of varying end restraints in order to differentiate the behavior of compression members with and without the additional resistance produced by neighboring tension members. The fundamental designs of the two primary testing configurations were based on models shown in Figure 1.3 (a) and (b).

These models provide a simple representation of the effects that idealized end restraint conditions have on the behavior of web members. Figure 1.3 (b) suggests that the bottom chord and adjacent tension members in a truss provide zero out-of-plane rotational or translational restraint, essentially behaving as a roller support. In contrast, Figure 1.3 (a) demonstrates the restraining effects of adjacent tension web members by modeling these members as cables.

To explore the varying end restraint conditions, three different configurations were tested throughout the experimental program. The first is a physical representation of the model in Figure 1.3 (b), where the support at the top restricts all degrees of freedom except vertical movement of the member, and the bottom support behaves as a roller providing restraint only vertical translation. The initially proposed conceptual design for this configuration is shown in Figure 2.2 (a). The second model accounts for the effects of adjacent tension members by modeling them as cables and this preliminary design configuration is shown in Figure 2.2 (b).

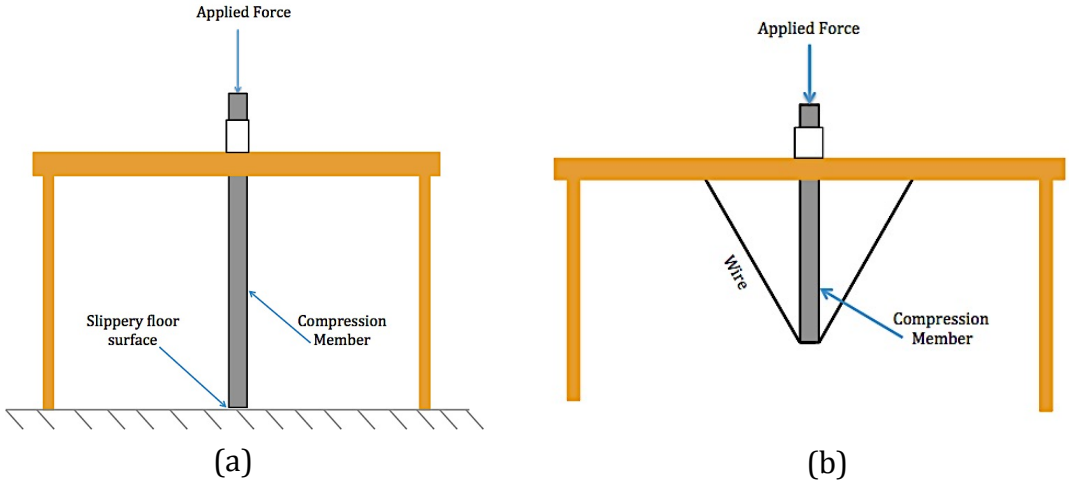

Figure 2.2. Preliminary design configurations for (a) roller and (b) tension cable models

The third testing configuration is shown in Figure 2.3. This setup was intended to provide an additional opportunity to observe the effects of adjacent tension members on both the neighboring compression members and members not directly impacted by the effects. Multi-member tests allow for further insight into how an entire system could be impacted by tensioning effects.

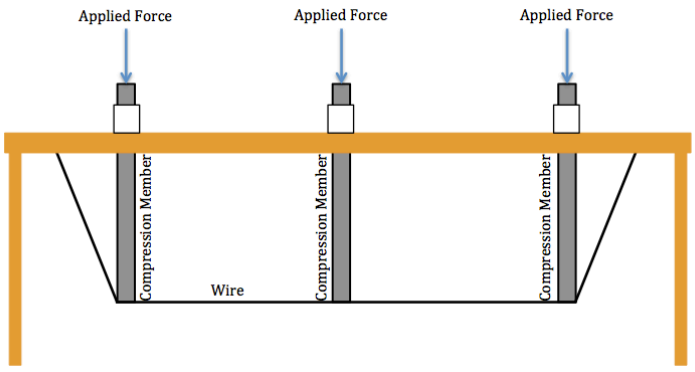

Figure 2.3. Preliminary design for triple-member model

2.1.1.1.1 Material Properties and Member Selection

One of the main limiting factors influencing the size of the experimental apparatus was the loading capacity of the laboratory testing machines available at Bucknell University. In order to scale the experimental apparatus to ensure that the loads necessary to buckle the test specimen for each configuration would be attainable, a plastic polymer was chosen for the experimental compression member. A half-inch diameter acrylic rod was determined to be the most suitable choice for the experiment and the rod lengths were sized accordingly by capping the maximum load necessary for buckling equal to approximately 50 pounds. This load cap falls well within the capacity of the Instron testing machine employed during the experimental testing program. The supporting calculations explaining the member sizing selections are located in Appendix A.

The slenderness ratio, *L/r*, of the test members was calculated using Equation (2.1) to ensure that the members were long enough that elastic buckling would be the controlling failure mode and that the Euler buckling equation, Equation (1.1), would apply. With these constraints, an *L/r* ratio greater than or equal to 100 was defined as the desired slenderness ratio. The slenderness ratios were calculated using equation (2.1), supporting calculations are located in Appendix A,

$$\frac{L}{r} = \frac{L}{\sqrt{\frac{I}{A}}} = \frac{L}{\left(\frac{R}{2}\right)} \geq 100 \qquad \text{Eq. (2.1)}$$

where: *r* is the radius of gyration of the section, *L* is the member length, *I* is the moment of inertia, *A* is the cross sectional area, and *R* is the radius of the section.

In order to mitigate potential sources of error resulting from variability in material properties between the manufacturers specification and the physical samples, the necessary element properties were investigated. A plastic flexural three-point bending test was performed, according to the American Society for Testing and Materials (ASTM) D790 Standards for Reinforced and Unreinforced Plastics, to determine the modulus of elasticity (ASTM, 2002). This test was done using the Instron 3366 testing machine shown in Figure 2.4. This Instron machine is controlled through an associated computer program, BlueHill, which has a variety of preprogramed testing parameters that can be applied and modified for any configuration.

Figure 2.4. Instron 3366 testing machine

To perform each of the five tests, 8-inch sections of the half-inch diameter acrylic rod were cut and placed in a three-point bending fixture, with a 4-inch support distance

within the load platform of the Instron machine. Figure 2.5 shows a schematic of the loading configuration applied to the specimen during the three-point bending test.

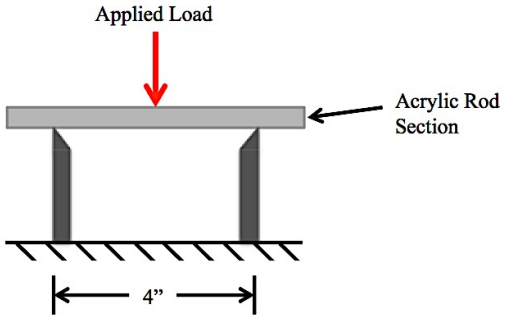

Figure 2.5. Schematic of three-point bending test

During a three-point bending test, a point load is applied to the middle of the test specimen until the testing machine measures a maximum strain of 5.0% (ASTM, 2002). Once this deflection is detected, the load is removed and a value for the flexural modulus is calculated and output by the control system. A summary of the statistical data collected from four trials of the three-point bending test can be found in Table 2.1.

Table 2.1. Summary of Statistical Data collected from 3-point Bending Tests

	Flexural Modulus (Modulus of Elasticity) *E* (ksi)
Minimum	421.2
Maximum	436.2
Mean	429.0
Standard Deviation	6.14
Variance	28.31

From these tests, the flexural modulus, *E*, of the test specimen is most accurately measured to be 429,000 psi, slightly lower than the 450,000 specified by the manufacturer. This value was used in place of the manufacturer's specification for all associated calculations.

Once the material selection and member sizing was completed, an initial rendering of the roller (shown in Figure 2.6) and three-member (shown in Figure 2.7) apparatus designs were completed using SOLIDWORKS (www.solidworks.com), a solid modeling computer-aided drafting (CAD) system.

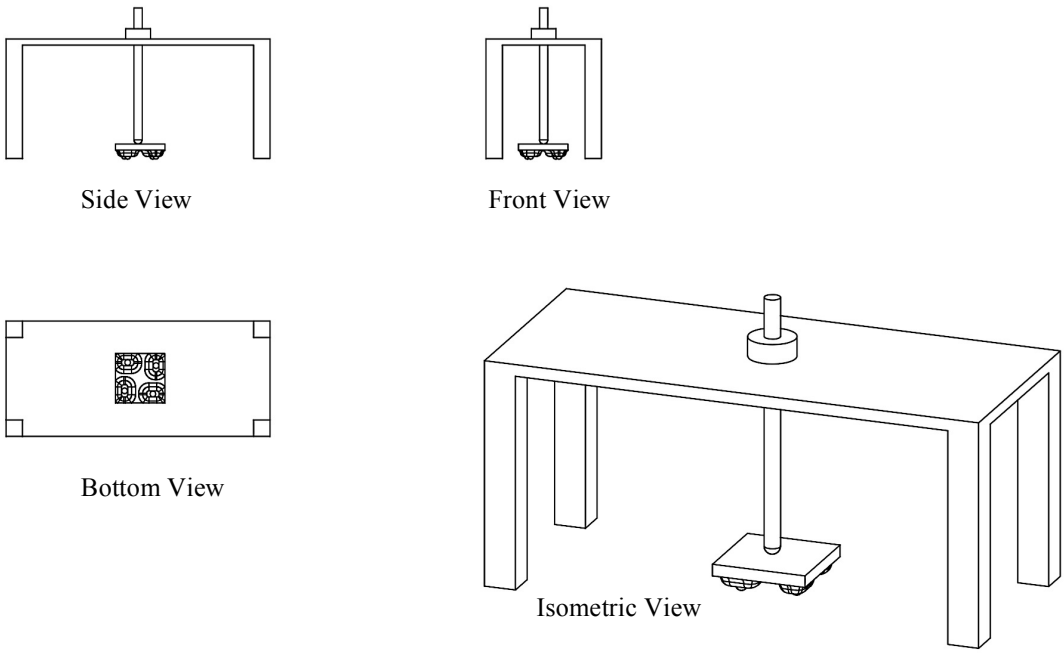

Figure 2.6. Rendering of preliminary design for roller apparatus

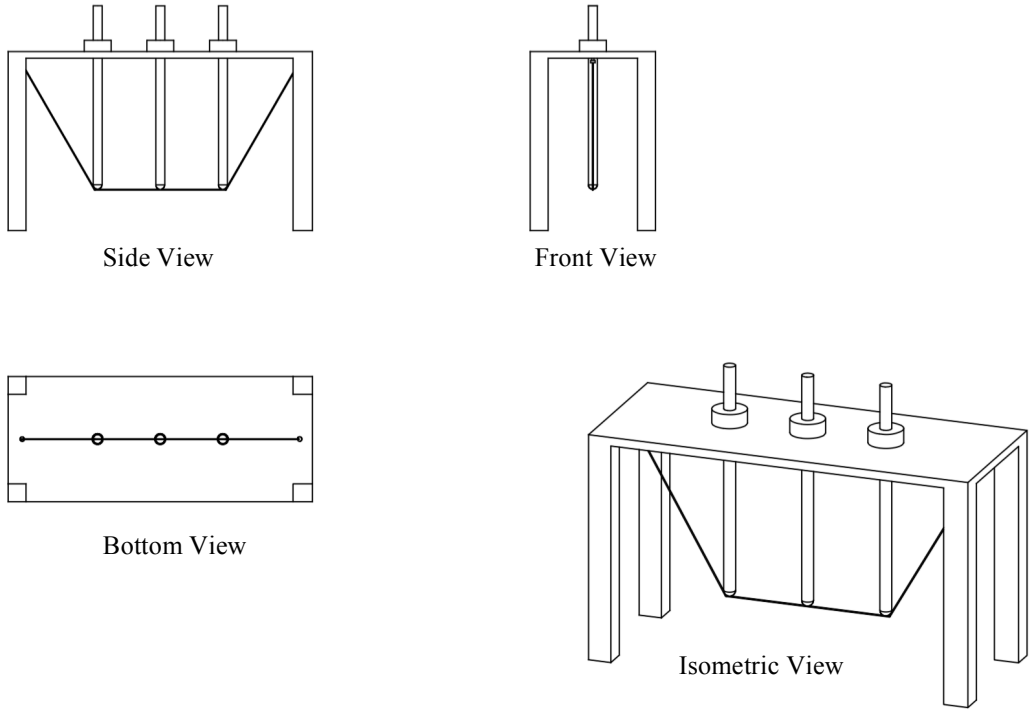

Figure 2.7. Rendering of preliminary design for three-member test apparatus

Using these preliminary designs, material was selected for each design component and is described in the following section.

2.1.1.2 Construction and Calibration Testing

In order to ensure accurate results, precise construction and calibration testing were required for the experimental testing apparatus. The primary components that required detailed attention are the supports which included (i) frictionless collars that restrict rotation and translation in all degrees-of-freedom except for vertical movement at the top, and (ii) a roller support that only restrains movement in the vertical direction at the

bottom of the column. Additionally, accurate alignment of the test members and the cable support level was very important. The effects of a deviation between the elevation of the bottom of the collar and the level of the cable connection was explored to determine the potential impact on the buckling behavior of the compression members and the accuracy of the collected results (Section 2.3.1.2).

2.1.1.2.1 Support Construction

Frictionless Roller Support

Ensuring a frictionless support was a priority in the construction of the experimental apparatus. Any degree of friction developed by the roller support would alter the critical buckling load thereby impacting the back-calculated effective length factor, *K*. Through a trial and error process, the finalized roller design was established; a photo is provided in Figure 2.8 and a detailed schematic of the design can be found in Appendix B. It consists of four ¾ inch diameter loose ball bearings that sit in-between two square metal plates each with two smooth notches to keep the balls from rolling out during testing. The acrylic rod was sanded to a hemisphere at its support end and a steel tip was inserted into the bottom to eliminate the possibility of the member tip flattening after repeated loadings, which could result in undesired rotational restraint.

Figure 2.8. Experimental Roller Apparatus Final Design

Frictionless Vertical Collar

The second important design feature was the collar at the top of the column, which prevents rotation and translation in all directions with the exception of vertical movement. This was designed through the incorporation of a flange mounted linear bearing that allows unhindered vertical movement while restraining all other degrees of freedom. As shown in Figure 2.9, three, half-inch diameter linear bearings were used in the apparatus.

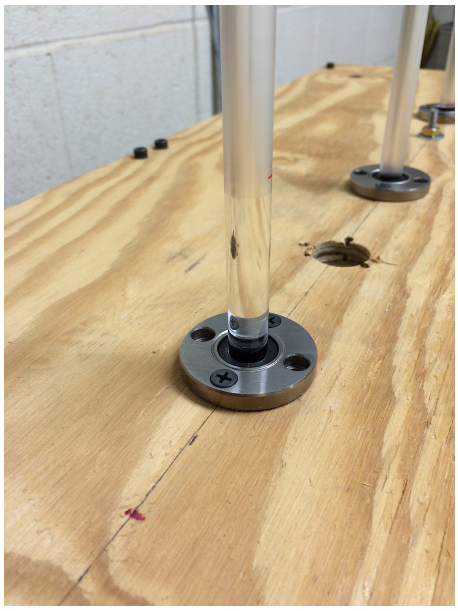

Figure 2.9. Linear bearing collar

Connections for Tension Cable

The construction of the cable model apparatus and three-member configuration required precise dimensioning to eliminate any undesired effects resulting from varying member length and differing heights of the cable supports. The impact of a variation in support height between the bottom of the vertical bearing and the cable connections to the wooden table will be explored in Section 2.3.1.2.

Ensuring precise measurement of the member length for the cable-buckling test required constant adjustments during construction and calibration testing. Two 1-inch diameter eyebolts were used for the connection between the cables and the table apparatus, as shown in Figure 2.10. Initially, the design intended to attach the loops created at the end

of the cable through the eyebolt. However, once the impacts of the variation between cable support height and the bottom of the column support were explored, as will be shown in Section 2.3.1.2, washers were used instead to raise the cable to the necessary elevation, thereby matching the bottom of the vertical ball bearing collar.

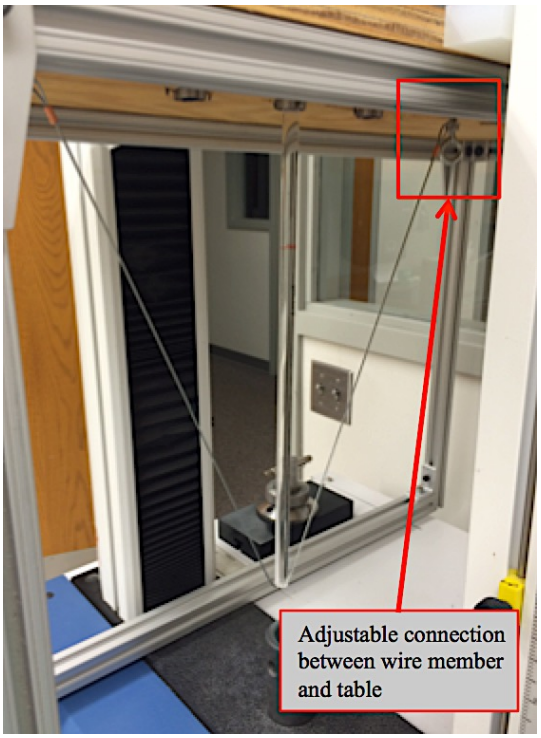

Figure 2.10. Tension model with connection to cable highlighted

Bracing for Triple-Member Test

The triple-member configuration created a unique issue that arose during construction and calibration testing (Figure 2.11). Due to the flexibility of the experimental compression members, the inward forces created by the initial tensioning of the cable caused the compression members to bend inward. This issue was corrected through the

addition of two, half-inch thick steel, metal spacers that were placed between the bottom ends of the compression members.

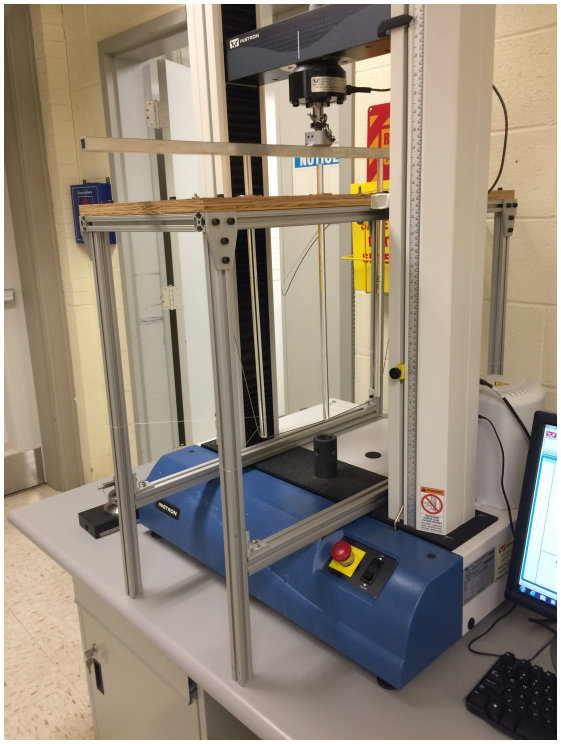

Figure 2.11. Triple-member system during construction

2.1.1.2.2 Calibration Testing

The results of the computational analyses (Section 2.3.2.2), along with results of the governing differential equations (Section 2.2), provide the anticipated buckling loads for the experimental testing configurations. During the calibration phase of this research, two single member tests were completed and the necessary adjustments were made in order to ascertain the accuracy of the apparatus and to troubleshoot problems within the test program.

2.1.1.3 Experimental Testing Procedure

The experimental testing program consisted of running trials on several buckling configurations. After initial setup and proper installation of the testing table into the Instron machine, the procedure began with a test run of the computer-buckling program to ensure that the appropriate parameters were input. Tests were then be run in groups of four to five trials using the same member. Between each trial, the test specimen was rotated 90 degrees to prevent an imperfection from developing in one direction due to repeated loading and buckling in the same manner. The triple-member test required an additional metal bar (seen in Figure 2.11) across the top of the compression members to distribute the load from the central loading point, this can be seen in Figure 2.11.

The Instron testing machine has the capability to perform a variety of loading conditions with different testing parameter inputs. For all three configurations a compression test was used with varied testing speeds dependent on the expected critical buckling load. The speed varied from one inch per minute to five inches per minute dependent on the test. Additional inputs include specimen properties, associated end of test signal, and output parameters. For the buckling tests, the test was programed to stop at a 10% decrease in load. The output of each test included a load versus extension graph with all data recorded in an accompanying spreadsheet.

2.1.2 Results

2.1.2.1 Introduction

The experimental results collected throughout the course of this study provide insight into the restraining effects that tension members may have on compression web members within truss systems. A simple scaled model representative of an inverted king post truss was constructed as a means of studying this tensioning behavior in its simplest form. Overall, three different experimental configurations were tested, each run with multiple trials to avoid the collection of flawed data.

2.1.2.2 Roller Model

The roller model consisted of a roller restraint at the bottom of the member (providing only vertical translational support) and a vertical ball bearing collar at the top (preventing rotation and translation in all directions with the exception of vertical translation). Buckling loads were measured by running a compression test using the Instron testing machine. Euler's buckling equation, Eq. (1.2), was then applied so that a *K*-factor could be back-calculated for each trial. Figure 2.12 shows one data set produced by the Instron testing software. The associated compressive strength, P_{cr}, and calculated effective length factors are shown in Table 2.2.

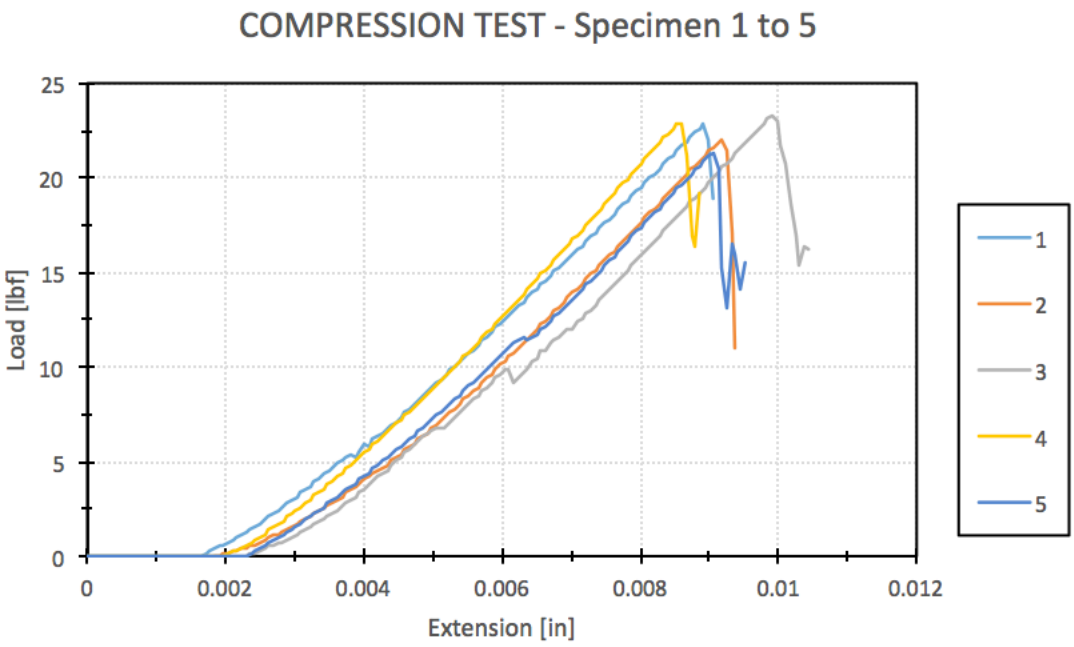

Figure 2.12. Data collected from Instron buckling tests of roller configuration

Table 2.2. Experimental Results from Roller Configuration

P_{cr} (lb)	*K*-factor
22.8	1.97
22.6	1.98
21.1	2.05
21.9	2.01
23.1	1.96
22.3	**1.99**

The buckling load and associated *K*-factor values found in the last row of Table 2.2 show the average of the collected data from that trial. Additional experimental data can be found in Appendix C. Figure 2.13 shows the resulting buckled shape of the experimental member.

Figure 2.13. Roller apparatus before (left) and after (right) buckling

2.1.2.3 Compression Cable Model

The simulated compression cable model was designed to explore the impacts of adjacent tension members on the buckled shape of compression web members. This configuration consisted of a compression member supported by a cable, as detailed in Section 2.1.1.2.1. Buckling loads were found by running a compression test using the Instron testing machine and back calculated effective length factor values were determined using Eq. 1.2. The graph in Figure 2.14 shows the output produced by the Instron testing machine, which results from one set of tests using the cable testing apparatus.

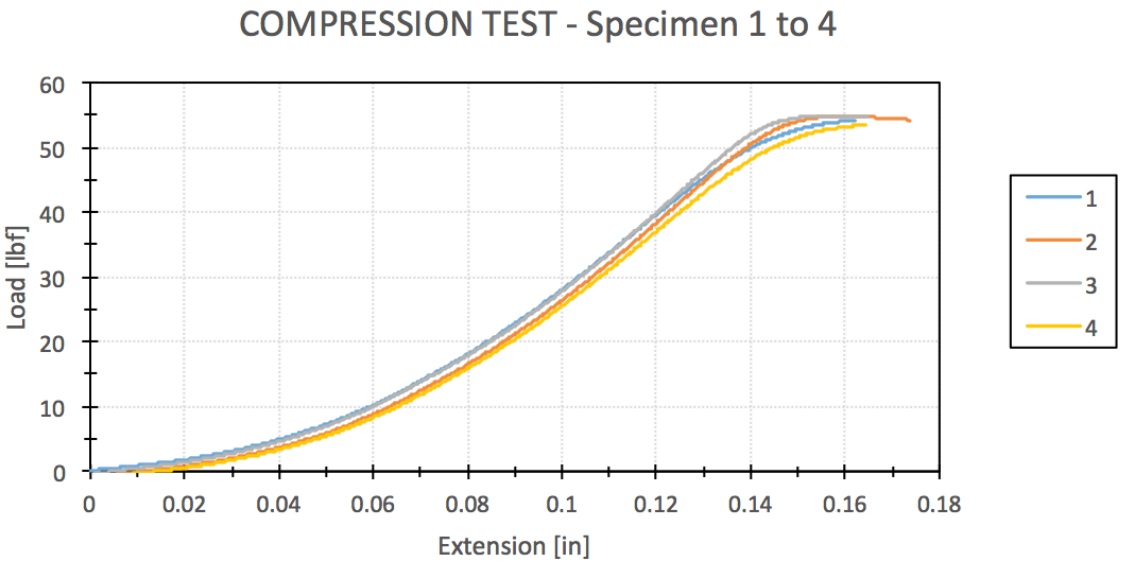

Figure 2.14. Data collected from Instron buckling test of cable apparatus

The associated buckling strength data and back-calculated effective length factors for the test results in Figure 2.14 are provided in Table 2.3.

Table 2.3. Experimental Results from Tension Cable Configuration

P_{cr} (lb)	***K*-factor**
51.6	0.99
49.0	1.02
44.0	1.07
53.0	0.98
52.3	0.99
50.7	**1.00**

The buckling load and associated *K*-factor in the last row of Table 2.3 show the average of the collected data from that set. Additional experimental data can be found in Appendix C. Figure 2.15 shows the resulting buckled shape of the experimental member.

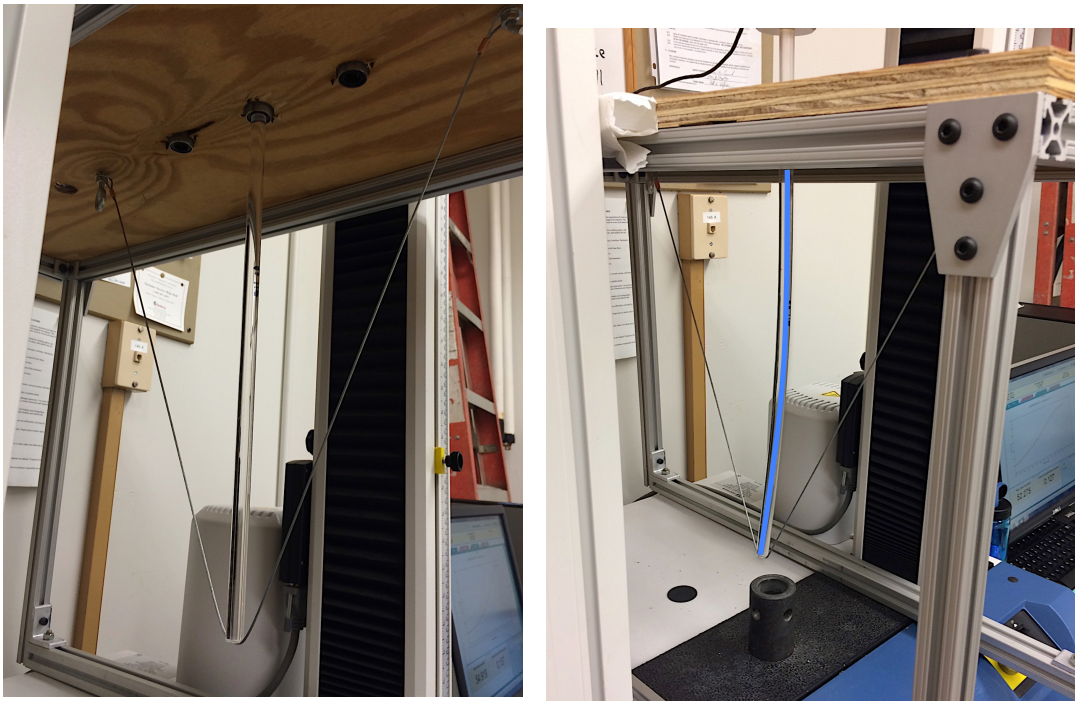

Figure 2.15. Cable apparatus before (left) and after (right) buckling

2.1.2.4 Triple-Member Model

The triple-member model provides insight into how a system behaves in which members are required to share the tensioning effects. This configuration consisted of three compression members supported in the system using a continuous cable. In order to prevent bending of the outer compression members during the tensioning of the cable, two half-inch thick steel, metal braces were added.

Due to the increased friction that developed between the bottom of the compression members and the cable within the apparatus, compression testing of this configuration was not completed in the same manner as the previous two studies. The system was loaded manually within the Instron testing machine until the two outer compression members buckled, leaving the central member untouched. The behavior of this system will be discussed further in Section 2.3.2.2.

2.1.3 Limitations

The results presented in this section of the thesis are limited by several factors associated with the experimental nature of the research. The largest factor affecting the applicability of the results to full-scale truss systems is the size and loading system of the experimental apparatus. The apparatus simulates the behavior of an inverted king post truss, which generally consists of only one or two web members. Larger trusses used in building design can have dozens of web members, leaving an amount of uncertainty when applying the results of this experimental research to a larger scale. Section 2.3.1.4 addresses the application of these results to larger scale systems. Variation of the loading application on the experimental apparatus is a parameter that, given the capacity of the available laboratory equipment, could not be altered. Future research should be performed with a variation of loading conditions in order to explore how it may impact the results presented in this thesis.

Additional uncertainty lies within the construction and behavior of the materials used in the experimental configuration. These results are analyzed under the assumption that the linear bearings used as the collars allow for frictionless vertical movement and completely restrain any rotational tendencies of the member. The constructed roller support is also assumed to act as a frictionless surface allowing the member to move in any translational direction. Obviously, any variation in these conditions will impact the results.

2.2 Governing Differential Equations

The focal point of this research is on the additional, unaccounted effects of tension members on the buckled shape of compression members. Lee's (2013) research suggested that the restraining effects produced by tension members impacts the buckled shape largely due to the alignment of the resisting force that develops with the addition of tension members, which in these studies is modeled as cables (Lee, 2013). Figure 2.16 shows the proposed resulting buckled shapes and alignment of the critical buckling load with respect to columns with and without the addition of tension members. In other words, these are the theoretical out-of-plane results for the systems shown in Figure 2.2

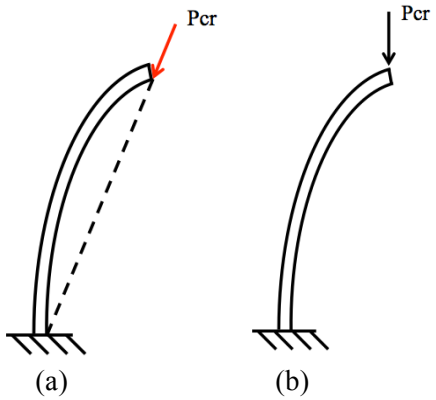

Figure 2.16. Resulting buckled shapes, with and without the additional restraint from tension members

The following two derivations work through the governing differential equations to solve for the Euler critical buckling load of each system, all in an effort to determine the respective effective length K-factors.

2.2.1 Case 1: Fixed-Free (Prove K = 2.0)

The fixed end of the column, as shown at the bottom of Figure 2.17 (a), is restrained in all translational and rotational directions. At the free end, the column is unrestrained in all degrees-of-freedom. When the column is subjected to a compression load on the free end, the resulting buckled shape is shown in Figure 2.17 (b). As a result of the flexure that occurs, a bending moment, *M(x)*, develops in the member.

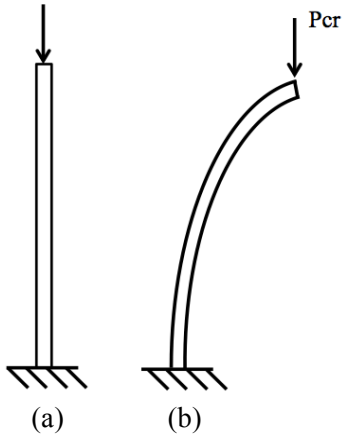

Figure 2.17. Fixed-Free column (before and after buckling)

At a distance *x* from the point of loading, the external moment caused by the load, P_{cr}, can be equated to the internal moment, *M(x)*, as shown in the free body diagram in Figure 2.18. The external moment is a function of the load and the lateral deflection, *v(x)*, at a distance *x* along the length of the member as shown in Figure 2.18.

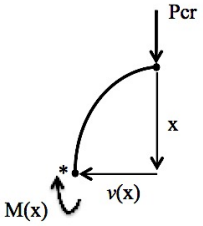

Figure 2.18. Free body diagram at distance *x* from load application

Performing an equilibrium analysis by summing the moments at the location labeled, *, on the free body diagram shown in Figure 2.18 produces

$$\sum M_* = 0 \tag{2.2}$$

$$-M(x) - P_{cr}\, v(x) = 0 \tag{2.3}$$

$$M(x) + P_{cr}\, v(x) = 0 \tag{2.4}$$

Substituting the moment-curvature relationship

$$M(x) = EI\, \frac{d^2v}{dx^2} \tag{2.5}$$

results in the following linear differential equation

$$EI\frac{d^2v}{dx^2} + P_{cr}v = 0 \quad , \tag{2.6}$$

which can be simplified to the following form:

$$\frac{d^2v}{dx^2} + \frac{P_{cr}}{EI}v = 0 \quad . \tag{2.7}$$

The solution to Equation (2.7) given that it is a linear homogeneous differential equations. In order to simplify Eq. (2.7), the following notation is implemented

$$w = \sqrt{\frac{P_{cr}}{EI}} \quad . \tag{2.8}$$

After substitution into Equation (2.7),

$$\frac{d^2v}{dx^2} + w^2v = 0 \quad . \tag{2.9}$$

The standard solution to this type of differential equation is in the form of $v(x)=e^{mx}$. When applying this to Eq. (2.9), *m,* for this application equals $\pm iw$. The general solution to Eq. (2.9) is this

$$v(x) = C_1e^{iwx} + C_2e^{-iwx} \tag{2.10}$$

Using the following Euler identity

$$e^{\pm iwx} = \cos(wx) \pm i\, sin(wx) \tag{2.11}$$

this general solution maybe rewritten as

$$v(x) = A_1 \sin(wx) + A_2 \cos(wx) \quad . \tag{2.12}$$

In order to determine the values of the constants A_1 and A_2, the following boundary conditions representing the fixed-free column in Figure 2.17 must be applied:

$$v(x = 0) = 0 \tag{2.13}$$

$$v'(x = L) = 0 \tag{2.14}$$

Applying the first boundary condition, $v(x=0)=0$, results in a value of A_2 as shown below

$$0 = A_1 \sin 0 + A_2 \cos 0 \quad . \tag{2.15}$$

$$A_2 = 0$$

To apply the second boundary condition, the derivative of $v(x)$ must be determined as shown below:

$$\frac{d}{dx} v(x) = \frac{d}{dx} [A_1 \sin(wx)] \tag{2.16}$$

$$v'(x) = wA_1 \cos(wx) \tag{2.17}$$

Employ the boundary condition, $v'(x=L)=0$, results in:

$$v'(x = L) = 0 = wA_1 \cos(wL) \tag{2.18}$$

$$wA_1 \cos(wL) = 0 \quad . \tag{2.19}$$

This can be satisfied in the following two ways

$$wA_1 = 0 \ , or \tag{2.20}$$

$$\cos(wL) = 0 \tag{2.21}$$

The first solution is the trivial solution and the second solution can be satisfied with

$$wL = n\frac{\pi}{2} \tag{2.22}$$

where, n = 1, 3, 5 … The smallest root is $n=1$, and corresponds to the lowest buckling mode. Substituting

$$L\sqrt{\frac{P_{cr}}{EI}} = \frac{\pi}{2} \quad . \tag{2.23}$$

into Equation (2.8) yields

$$P_{cr} = \frac{\pi^2 EI}{4L^2} \quad . \tag{2.24}$$

This can then be simplified into the proper form to match Euler's buckling equation, Equation (1.1), which is given by

$$P_{cr} = \frac{\pi^2 EI}{(2L)^2} \tag{2.25}$$

From this solution of Euler's buckling load, it has been shown that a fixed-free column has an effective length factor of $K=2$.

2.2.2. Case 2: Fixed-Free with Cable Restraint (Prove K = 1.0)

In order to computationally determine the effects of tension members on the effective buckling length of columns, the previous differential equation solution was repeated assuming that the buckling force, P_{cr}, tracks the orientation of the tension cables as the column buckles (Figure 2.19).

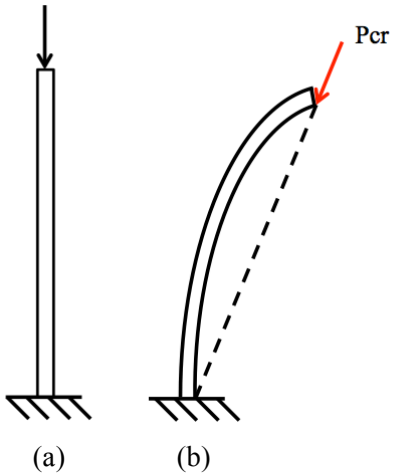

Figure 2.19. Fixed-Free with Cable Restraint Column System (before and after buckling)

The diagram in Figure 2.20 provides the notation that will be used in the following differential equation analysis. The critical buckling load, P_{cr}, is broken into x- and y-force components using the notation αP_{cr} and βP_{cr}, respectively.

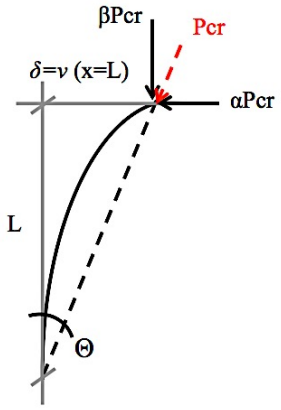

Figure 2.20. Diagram with defined notation

One major assumption integral to the following solution is the application of a small angle approximation. This means the following relationships hold true for θ, specified in Figure 2.20:

$$tan\theta \cong \theta \cong \delta/L$$

$$cos\theta \cong 1$$

$$sin\theta \cong \theta \cong \delta/L\,.$$

where δ = deflection as a function of the length and L = length of the column. Under this assumption, values for α and β can be determined using geometrical identities for sine and cosine resulting in the following:

$$P_{cr}cos\theta = \beta P_{cr} \tag{2.26}$$

$$\boldsymbol{\beta = cos\theta \cong 1} \tag{2.27}$$

$$\alpha P_{cr} = P_{cr}sin\theta \tag{2.28}$$

$$\alpha = sin\theta \cong \theta \cong tan\theta = \frac{\delta}{L} \tag{2.29}$$

$$\boldsymbol{\alpha = \frac{\delta}{L}} \tag{2.30}$$

The same procedure of equating the external and internal moments, as detailed for the fixed-free column, applies to the free body diagram shown in Figure 2.21. The associated free body diagram differs from the previous system due to the additional force component as shown in Figure 2.21.

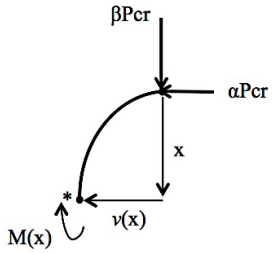

Figure 2.21. Free body diagram at distance *x* from load application

Performing an equilibrium analysis by summing the moments at the location labeled, *, on the free body diagram shown in Figure 2.21 produces

$$-M(x) + \alpha P_{cr} x - \beta P_{cr} v(x) = 0 \tag{2.31}$$

After substitution of the moment-curvature relationship and simplification, the governing differential equation is

$$EI\frac{d^2v}{dx^2} - \frac{\delta}{L}P_{cr}x + P_{cr}v(x) = 0 \tag{2.32}$$

or $$\frac{d^2v}{dx^2} - \frac{\delta}{L}\frac{P_{cr}}{EI}x + \frac{P_{cr}}{EI}v(x) = 0 \tag{2.33}$$

In order to simplify Eq. (2.33) further, following notation is implemented

$$\omega = \sqrt{\frac{P_{cr}}{EI}} \tag{2.34 (a)}$$

$$y = \sqrt{\frac{\delta}{L}} \tag{2.34 (b)}$$

With substitutions, Eq. (2.32) to becomes

$$\frac{d^2v}{dx^2} - y^2\omega^2 x + \omega^2 v(x) = 0 \tag{2.35}$$

This equation is a non-homogeneous linear differential equation, with a general solution of

$$v(x) = A_1 sin\omega x + A_2 cos\omega x + xy^2 \tag{2.36}$$

In order to solve for constants A_1 and A_2, the following boundary conditions associated with the tension-cabled column system in Figure 2.19 are applied

$$v(x = 0) = 0 \tag{2.37}$$

$$v'(x = L) = 0 \tag{2.38}$$

$$v(x = L) = \delta \tag{2.39}$$

Applying the first boundary condition, $v(x=0)=0$, defines the value of A_2 as

$$v(x = 0) = 0 = A_1 \sin(0) + A_2 \cos(0) + 0$$

$$\boldsymbol{A_2 = 0\ .}$$

In order to apply the second boundary condition, $v'(x=L)=0$, the derivative of $v(x)$ is taken, which results in

$$v'(x) = A_1 \omega cos\omega x + y^2 \tag{2.40}$$

Then, the second boundary condition can be applied to solve for A_1

$$v'(x = L) = 0 = A_1 \omega cos\omega L + y^2 \tag{2.41}$$

$$\boldsymbol{A_1 = \frac{-y^2}{\omega cos\omega L}} \tag{2.42}$$

Upon substitutions, the solution to the governing differential equation then simplifies to

$$v(x) = \frac{-y^2}{\omega cos\omega L} sin\omega x + xy^2 \tag{2.43}$$

Applying the third and final boundary condition, $v(x=L)=\delta$, results in

$$v(x = L) = \delta = \frac{-y^2}{\omega cos\omega L} sin\omega L + Ly^2 \tag{2.44}$$

$$\frac{\delta}{y^2} = -\frac{1}{\omega} tan\omega L + L \tag{2.45}$$

$$\frac{\delta}{\left(\delta/_L\right)} = -\frac{1}{\omega} tan\omega L + L$$

$$L = -\frac{1}{\omega} tan\omega L + L$$

$$0 = -\frac{1}{\omega} tan\omega L \tag{2.46}$$

By applying the small angle theory

$$tan\omega L = 0 = sin\omega L \quad . \tag{2.47}$$

and then smallest nontrivial solution to Eq. (2.47) is

$$\omega L = \pi \qquad . \tag{2.48}$$

substitution into Eq. (2.34(a)) and after simplification the critical buckling load, P_{cr}, can be computed as

$$L\sqrt{\frac{P_{cr}}{EI}} = \pi \tag{2.49}$$

$$P_{cr} = \frac{\pi^2 EI}{L^2} \tag{2.50}$$

From this solution of Euler's buckling load, it has been shown that a fixed-free with cable restrained column has an effective length factor of *K=1*.

2.3 Computer Analysis

Computer analyses was performed modeling the experimental apparatus to confirm the collected results and to further explore factors that may influence the result. The results

from these studies are intended to confirm the applicability of the experimental results to larger-scale truss systems and explore what factors could influence the conclusions being made from this research.

2.3.1 Methodology

2.3.1.1 Analysis of Experimental Models

In order to determine the accuracy of the experimental results, the models shown in Figure 2.22 were created in MASTAN2 (www.mastan2.com). These models simulate the behavior of the experimental apparatuses by replicating the end conditions of the roller and cable tests. The top connection of both models restricts translation and rotation in all degrees-of-freedom except vertical movement. The bottom of the roller model, as shown in Figure 2.22(a), only vertical restraint is provided, matching the idealized support condition modeled in the experimental apparatus. The cable model, Figure 2.22 (b), provides the idealized restraint condition through the connection to two cable elements. The triple-member test, shown in Figure 2.23, has similar connections at the top and bottom as the single cable test. Both cable members are supported at the same elevation of the top of the compression member by a pin and connected to the bottom of the compression member by a pinned connection.

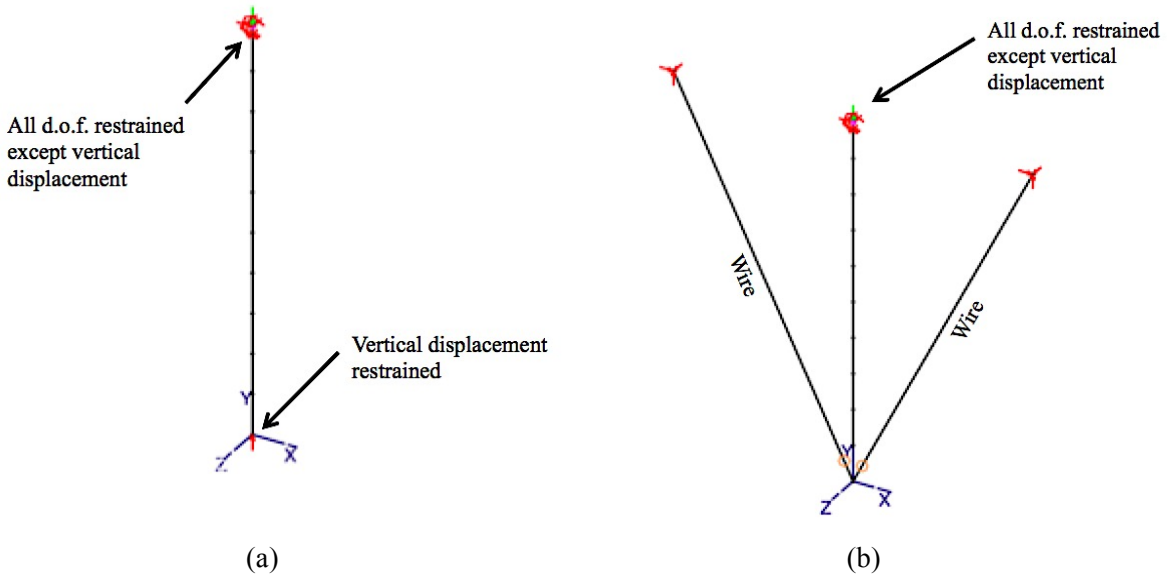

(a) (b)

Figure 2.22. MASTAN2 Models of preliminary behavioral testing with roller and cable models, respectively

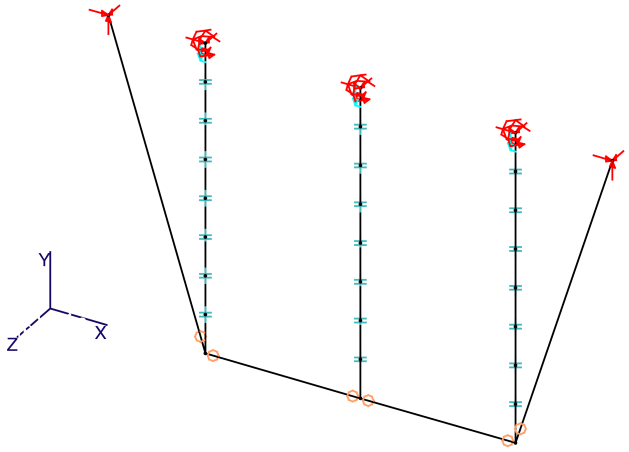

Figure 2.23. MASTAN2 Model of three-member system

The material and section properties used in these models correspond to the properties of the physical experimental apparatus and are provided in Table 2.4.

Table 2.4. Experimental member properties for computer analysis

Apparatus Configuration	**Length (in)**	**Area (in^2)**	**I_x (in^4)**	**I_y (in^4)**	**J (in^4)**	**E (psi)**
Compression Member in Roller Model: Figure 2.6 (a)	12.125	0.196	0.00307	0.00307	0.00614	429,000
Compression Member in Models with Tension Cables: Figure 2.6 (b)	16	0.196	0.00307	0.00307	0.00614	429,000
Cable	varies	0.00307	7.49e-7	7.49e-7	15e-7	29,000,000

For the single-compression member systems, a unit load was applied to the top of each compression member and an elastic critical load (Eigen value) analysis was performed on each of the computer models shown in Figure 2.22. By using a unit load, the buckling load factor would represent the buckling load value.

In order to simulate the actual loading of the triple-member system during the experimental testing, the computer model had to account for the differential loading that occurred due to the geometry of the system. During the experimental testing, a metal bar that laid across the tops of the members was loaded at one central location, which allowed the load to be distributed into the three members as the system adapted to the load. Modeling the computer system with three point loads at the top of the members would not be representative of the experimental loading, because it would induce the same force into every member, which was observed through the experimental system to not be the case. Instead, a unit differential settlement was applied to the top node of each

of the compression members to more accurately reflect the experimental loading condition described in Section 2.1.1.3.

2.3.1.2 Exploring Effects of Varying Support Height

During the construction phase of the experimental testing, the extent to which a vertical height difference, *ΔH*, between the lowest point of the linear bearing collar and the elevation at which the cable connected to the testing table, (Figure 2.24), was explored through an analytical study in MASTAN2.

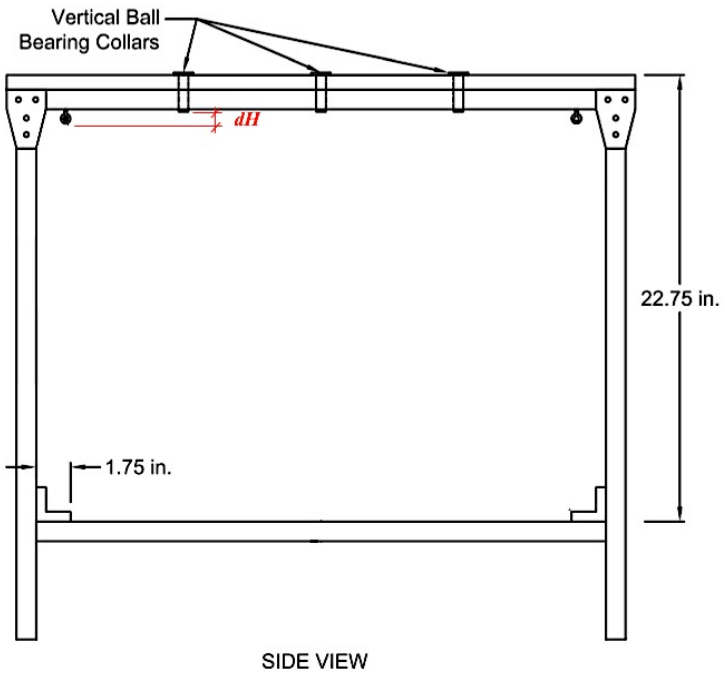

Figure 2.24. Schematic of cable testing apparatus, differential height, *ΔH,* labeled

The properties of the experimental configuration with tension cables (numerical values provided in Table 2.2) were used as the section properties for the model in MASTAN2. The other properties of the MASTAN2 model match those specified for the analytical cable model from Section 2.3.1.1. This structural analysis program has the ability to perform elastic critical load (buckling) analysis, of systems under any loading condition, to determine the critical buckling load. This latter value can then be used to back-calculate the effective length factor using Equation (1.2). Elastic critical buckling analyses were run on the model shown in Figure 2.25 while varying the height differential, ΔH, from zero inches to a one and a half inches.

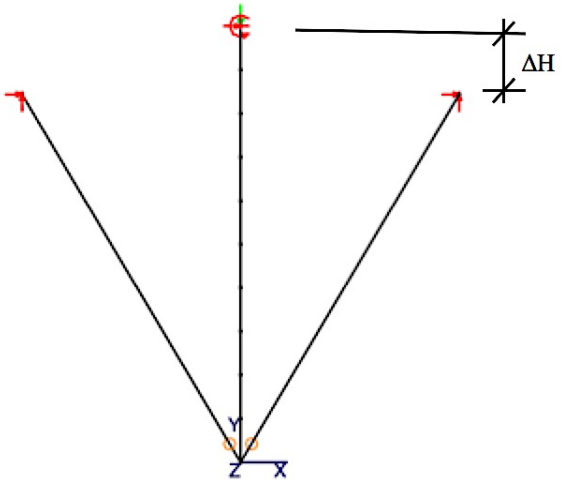

Figure 2.25. MASTAN2 model used to study the effects of varying support heights

2.3.1.3 Exploring Rotational Stiffness Requirements

In order to explore the effects of varying degrees of rotational stiffness that could not be physically tested due to the non-adjustable nature of the linear bearing collar, a

MASTAN2 study was performed using the models shown in Figure 2.26 (a) and (b). These models have the same material and section properties, and fixity conditions as those detailed in Section 2.3.1.1.

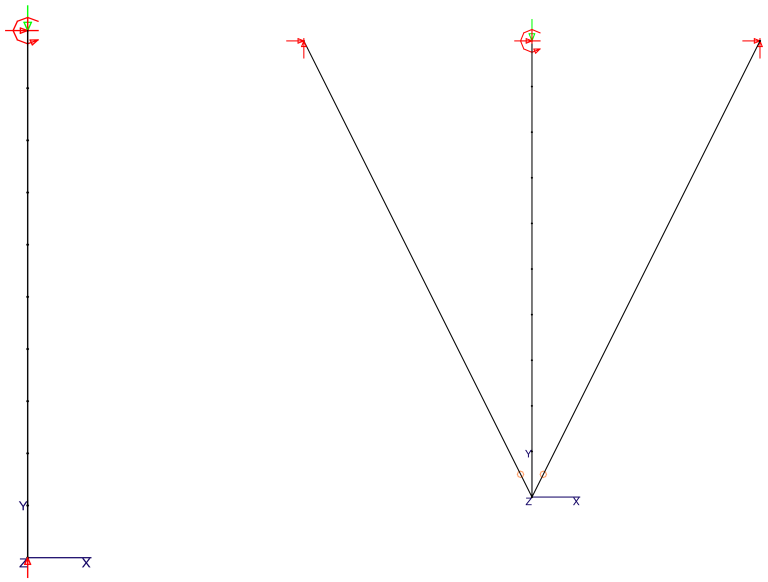

(a) (b)

Figure 2.26 (a) & (b). MASTAN2 models used for rotational stiffness study

Roller Model

Since the roller support at the bottom of the experimental apparatus, modeled in Figure 2.26 (a), does not restrict rotational movement in any direction, the only variations to be addressed within this system were through adjustments of the top connection (which was physically modeled using a linear bearing collar in the experimental apparatus). To observe the impact of the rotational stiffness of the top connection on the buckling load of the system, the two rotational-restraint conditions (Figure 2.27) were tested. These two

MASTAN2 models were loaded with a unit load and analyzed using elastic critical load (buckling) analyses.

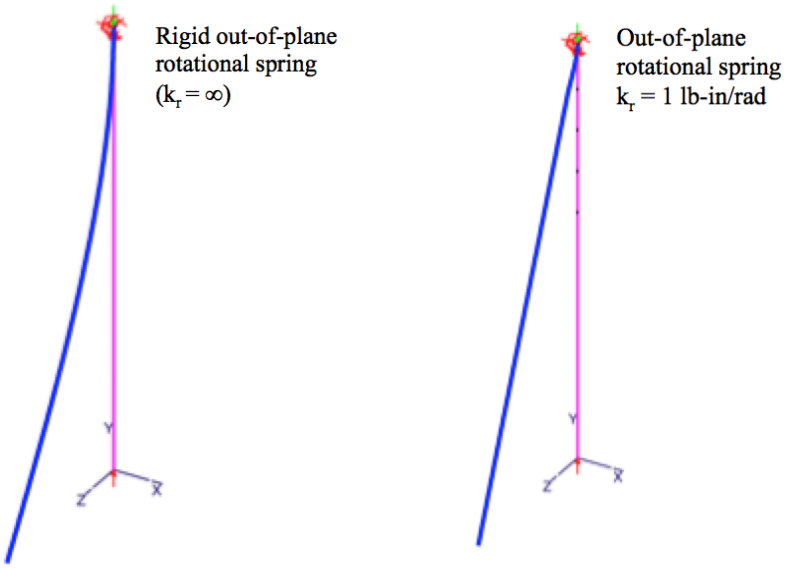

Figure 2.27. MASTAN2 Model of roller configuration with varying degrees of rotational restraint at top connection

Simulated Tension Member Model

The computational model designed to account for the tensioning effect through the addition of a cable chord can be included to provide opportunities to explore more variations of rotational resistance in both the top and bottom connections. The combinations of connection resistance in the top and bottom of this system can be found in Figures 2.28 and 2.29. The same loading method was applied to these models, with a unit force applied to the top of the compression member.

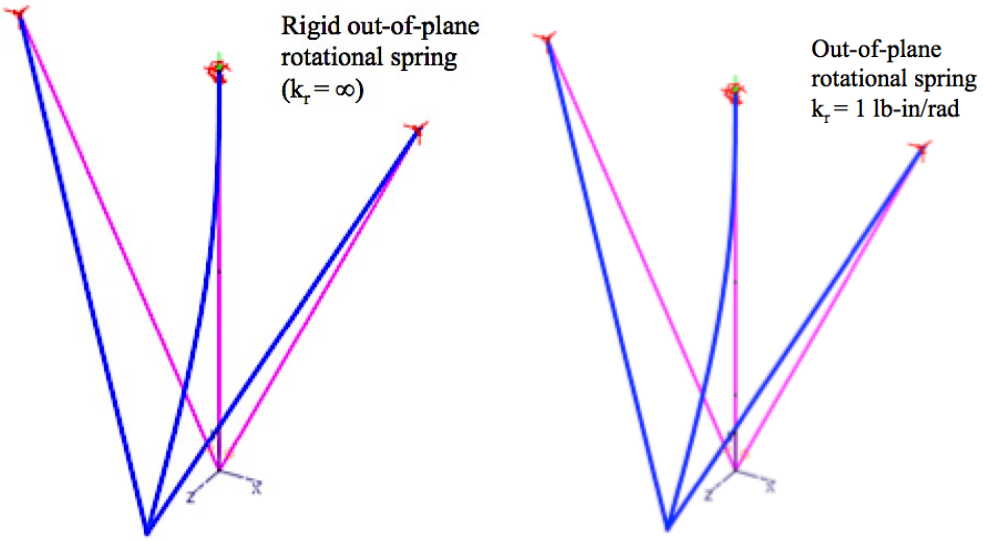

Figure 2.28. MASTAN2 Model of tension configuration with varying degrees of rotational restraint at top connection, zero rotational restraint at bottom

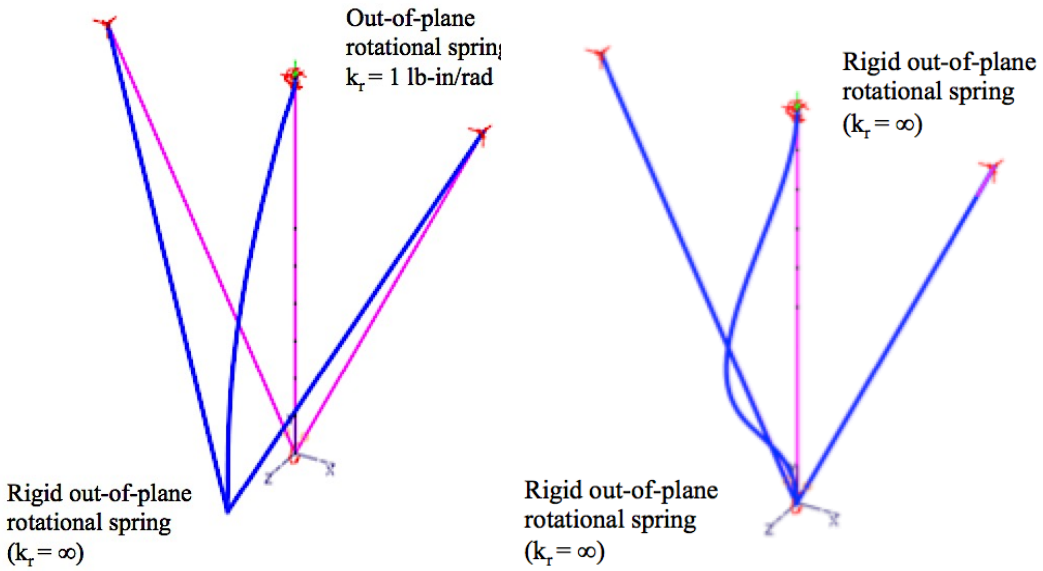

Figure 2.29. MASTAN2 Model of tension configuration with varying degree of rotational restraint at top and bottom connections

2.3.1.4 Application to a Full Truss System

The experimental configuration accounting for the additional rotational restraint from tension members has the same geometrical shape of an inverted king post truss, in which two tension members surround a compression member as shown in Figure 2.30. Similar three-member systems, comprised of a compression member surrounded by two tension members, can be found in larger trusses such as the modified Pratt truss examined in the computer analysis portion of this thesis (Figure 2.31).

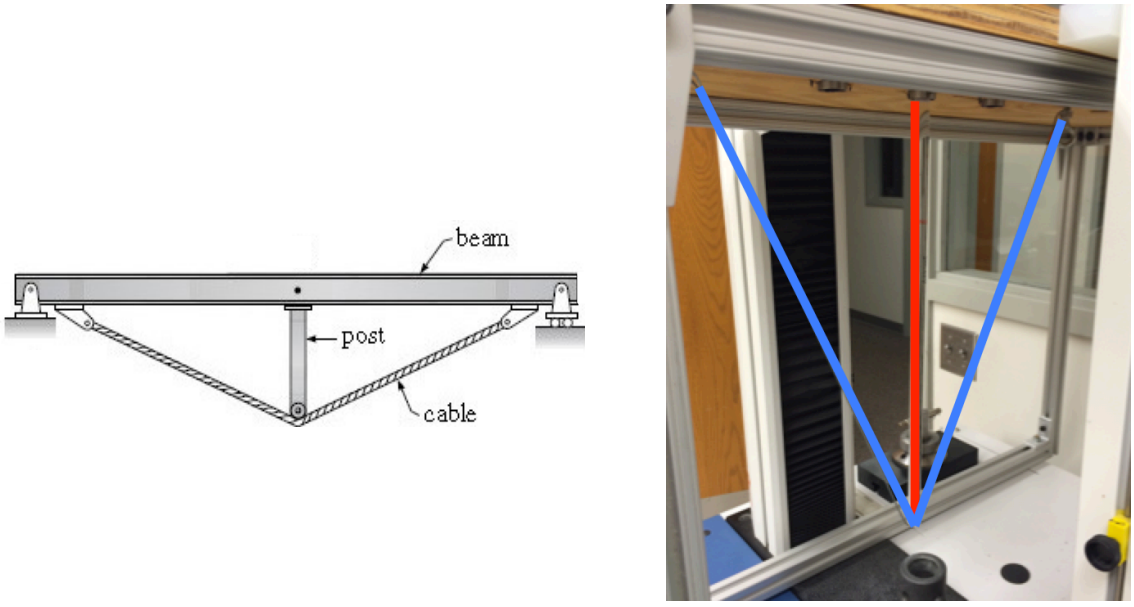

Figure 2.30. Experimental apparatus, right, comparison to king post truss, left (*citation)*

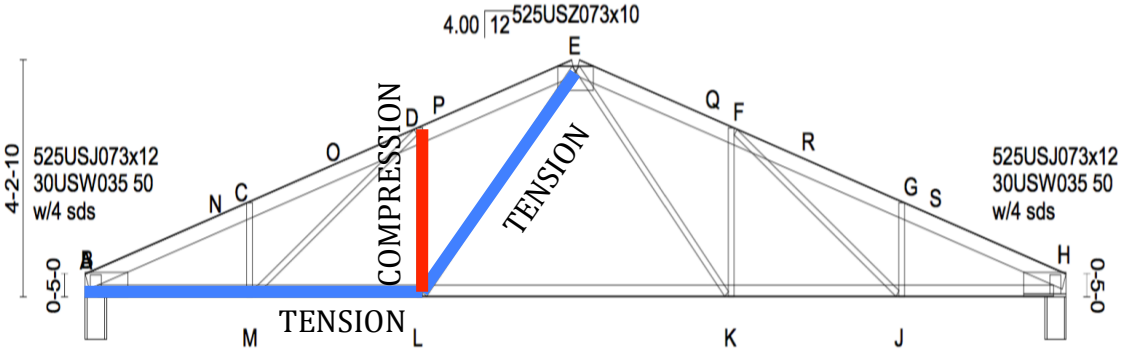

Figure 2.31. Identification of king post truss system within modified Pratt truss

While the experimental system constructed and analyzed throughout this research mirrors the geometry of an inverted king post truss, an additional computational study was performed to ensure that a rotated version of the system, similar to the one highlighted in Figure 2.31, would produce equivalent results. The MASTAN2 model shown in Figure 2.32 has the same material, section and geometrical properties as similar models of the tension member configuration in Section 2.3.1.1, with the exception of the elevation of the left support, which was lowered to the same level as the bottom of the compression member. A unit load was applied to the top of the compression member and an elastic critical load (buckling) analysis was run in MASTAN2 to determine the resulting buckling load.

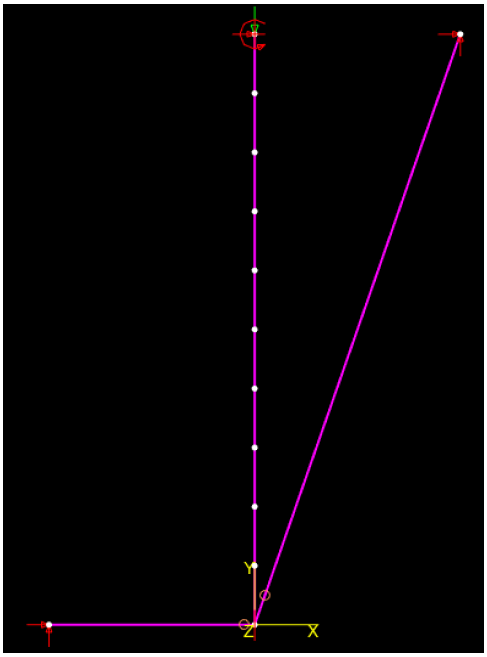

Figure 2.32. MASTAN2 Model Representative of king post system in larger truss

2.3.2 Results

2.3.2.1 Introduction

The results presented in this section include the findings from computer analyses of the experimental systems. Such results are essential in determining the accuracy of the experimental testing program and also provide a means of exploring alternative influential factors that were not physically tested.

2.3.2.2 Experimental Model Computational Results

Roller and Single-Member Cable Models

MASTAN2 elastic critical load (buckling) analysis of models representative of the physical experimental system were performed, yielding the results shown in Table 2.5. The resulting buckled shapes for each of the models are shown in Figure 2.33.

Table 2.5. Buckling Results of Experimental MASTAN2 Analysis Models

	Critical Buckling Load, P_{cr} (lb)	***K*-factor**
Roller model: Figure 2.6 (a)	22.1	2.0
Model with tension cables: Figure 2.6 (b)	50.7	1.0

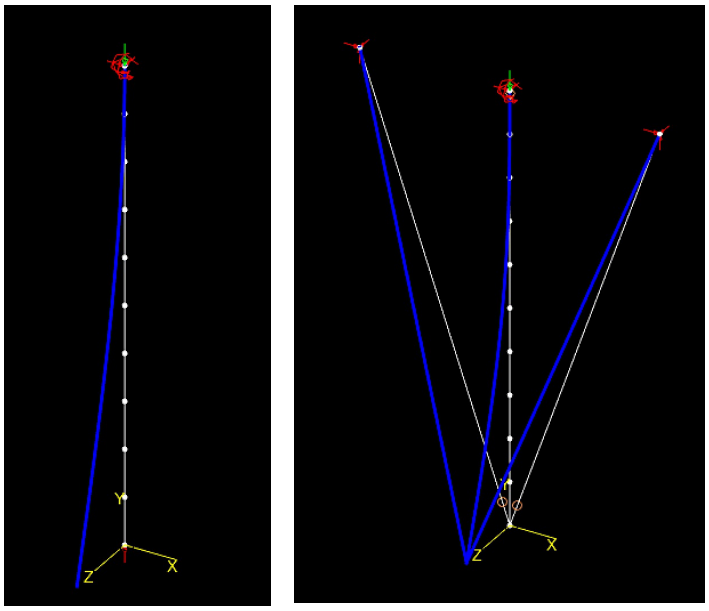

Figure 2.33 (a) & (b). Buckled shape of preliminary MASTAN2 models

Triple-Member Cable Model

The results of the MASTAN2 analysis of the triple-member system parallel the results observed in the experimental testing portion of this research. The resulting deflected shape diagram and axial force diagram are shown in Figure 2.34 and 2.35, respectively.

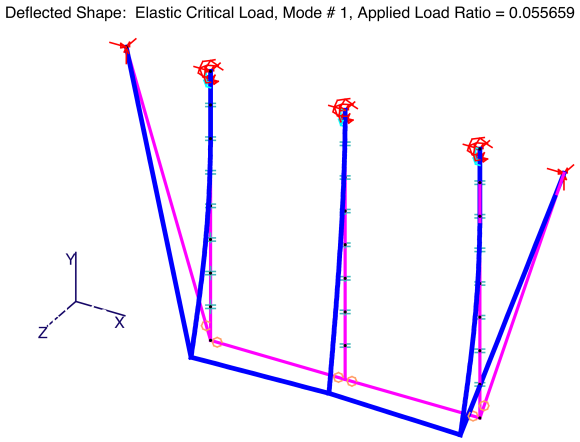

Figure 2.34. Triple-member system deflected shape diagram

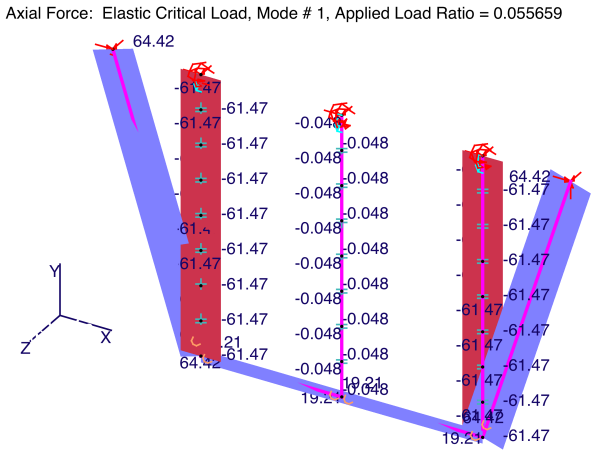

Figure 2.35. Triple-member system axial force diagram

The resulting behavior of the triple-member system, seen above in Figure 2.35, can be explained through a basic understanding of a zero-force member. The central web

member, by definition of a zero-force member, does not behave in tension or compression, which can be seen in the axial force diagram.

2.3.2.2 Varying Support Height

Figure 2.36 provides a summary of the collected results from this study. There is a clear linear correlation between varying support heights of both cables and the percent difference in the critical buckling load. As ΔH increases, meaning a larger distance between the support heights, the buckling load decreases increasing the percent difference between the expected critical buckling load and the resulting value.

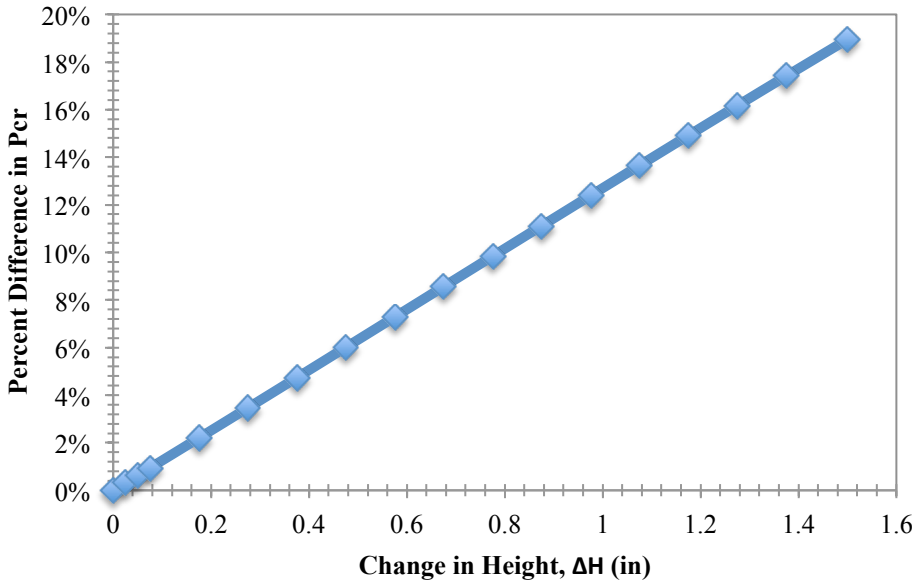

Figure 2.36. Study results of height variation between supports

From this study, the necessary accuracy of the apparatus construction became quite apparent, and required that the cable connection to the table occur at the same elevation as the bottom of the vertical journal bearing.

2.3.2.3 Rotational Stiffness

In order to further investigate the effects of varying degrees of end restraint within the experimental systems, models of such systems were analyzed in MASTAN2. The roller model from Section 2.3.1.1 was analyzed with varying degrees of rotational resistance provided by the top connection. The results of these analyses are provided in Table 2.6.

Table 2.6. Results of Varying Rotational Stiffness in Roller Model

	Rotational Resistance Provided by Top Connection		
Rotational Resistance Provided by Bottom Connection		**Rigid ($k_r = \infty$)**	**Rotational Spring (k_r = 1 lb-in/rad)**
	Free ($k_r = 0$)	P_{cr} = 22.1 lb K = 2.00	P_{cr} = 0.0822 lb K = 32.8

The tension model also provided the opportunity to vary multiple end restraint conditions and observe how their interaction affects the critical buckling load. The results of this study are shown in Table 2.7.

Table 2.7. Results of Varying Rotational Stiffness in Tension Model

	Rotational Resistance Provided by Top Connection		
Rotational Resistance Provided by Bottom Connection		**Rigid ($k_r = \infty$)**	**Rotational Spring (k_r = 1 lb-in/rad)**
	Only cable effects	P_{cr} = 50.7 lb K = 1.00	P_{cr} = 50.7 lb K = 1.00
	Rigid ($k_r = \infty$)	P_{cr} = 203.0 lb K = 0.50	P_{cr} = 51.2 lb K = 1.00

2.3.2.4 Application to Full Truss Results

The results of a MASTAN2 study of a model more closely mirroring the three-member system geometry found in the modified Pratt truss, which is studied more closely in Chapter 3, is shown in Figure 2.37. The resulting buckling load was 50.2 pounds with an associated effective length factor of 1.0, shows that the geometric configuration of the neighboring tension members does not impact the observed restraining effect.

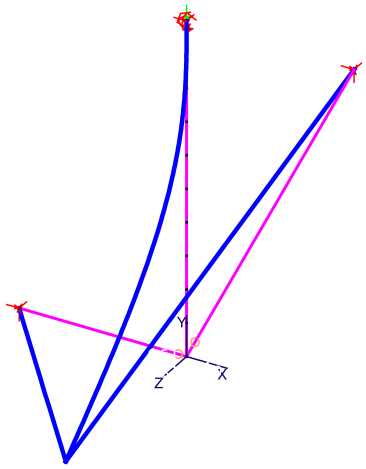

Figure 2.37. MASTAN2 model of adjusted cable configuration, with buckled shape

CHAPTER 3: ANALYSIS OF A MODIFIED PRATT TRUSS

One of the motivating factors behind performing this research began with the question of whether a *K*-factor of less than 1.0 could be used in the design of the compression web members in a modified Pratt truss (Figure 3.1). This truss provided an opportunity to transition from the scaled results of the experimental testing, to a computer simulation of a full-scale truss. The section properties of the members were specified by the manufacturer and are provided in Appendix D. Additional specifications were provided by the manufacturer and will be addressed in the description of the MASTAN2 model of the system.

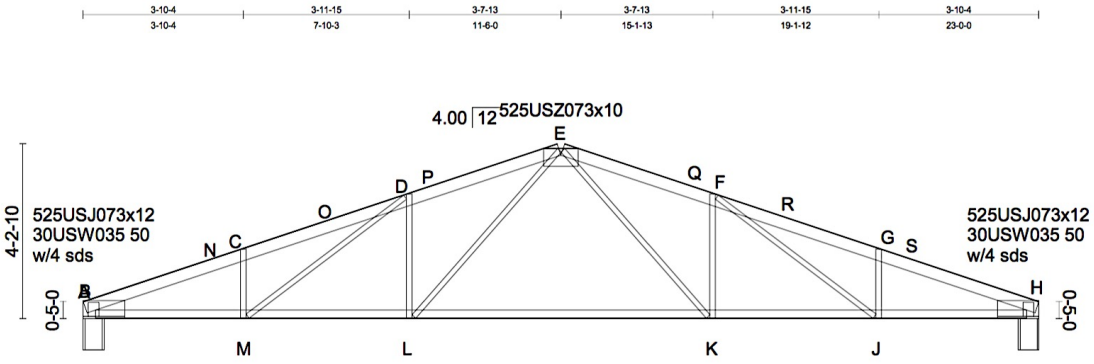

Figure 3.1. Modified Pratt truss analyzed in computational studies

Computer analysis is the second major component of this research, and was used to explore the resisting effects of adjacent tension members within a larger truss system. This chapter discusses the computational analysis methods applied in these studies.

The primary MASTAN2 model used throughout this computational study is shown in Figure 3.2. The geometric properties match those specified by the manufacturer in Appendix D. The manufacturer also provided the spacing of out-of-plane bracing as six feet on center uniformly spaced along the bottom chord. The top chord was assumed be continuously braced by the roof deck. All member segments are subdivided into four elements in an effort to provide accurate results. Each web member has continuous torsional restraint along the length. The top and bottom chords are also subdivided, but the torsional restraint is continuous along the entire length of each chord, which was modeled by providing continuous restraint even through the connection joints. The truss was assumed to be simply supported, with translation in the y- and z- directions are restrained at both ends and translation in the x- direction restrained at the center of the bottom chord.

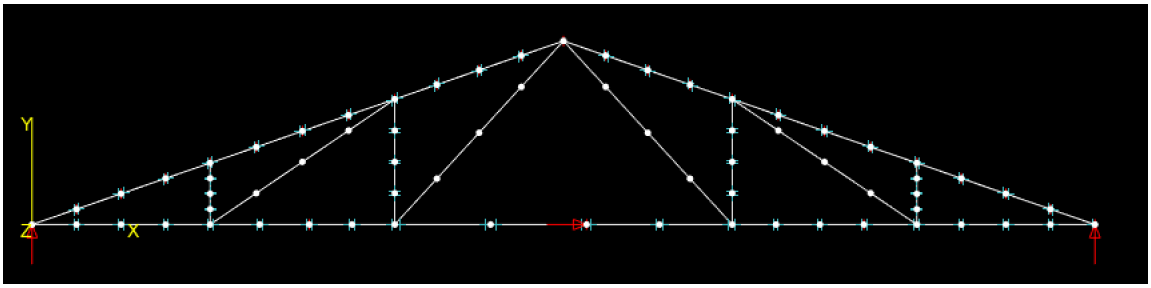

Figure 3.2. Full truss model in MASTAN2

Preliminary computer analyses, with a simple uniform gravity load on the upper chord, was performed to determine the behavior of all of the members in the truss (Figure 3.3). From this analysis it was possible to select the compression member of interest, which would be studied as the primary buckling failure member (Figure 3.4).

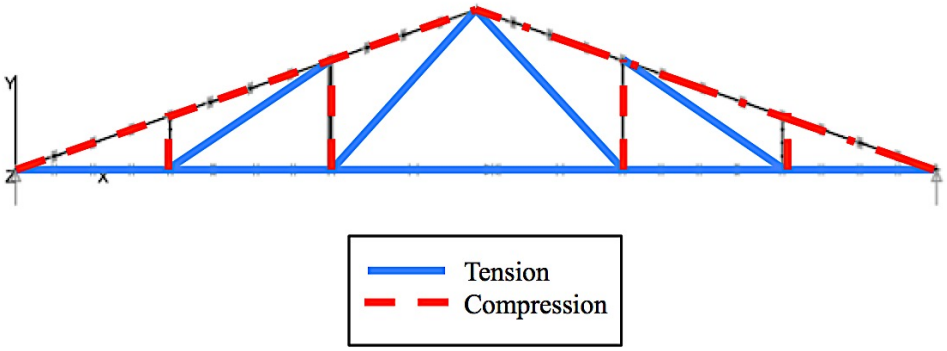

Figure 3.3. Behavior of truss members under uniform gravity load

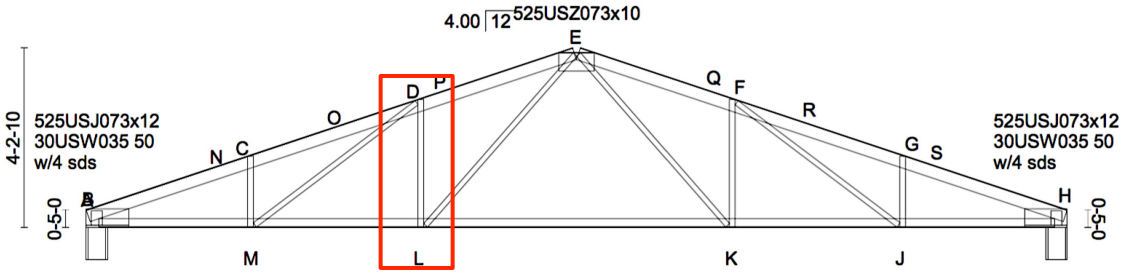

Figure 3.4. Truss model with compression web member of interest boxed

3.1 Equivalent Column Method

Solely through the use of elastic critical (buckling) analysis, it was not possible to determine a definitive source of failure resulting from an applied uniform gravity load due to the possibility of torsional failure. In order to determine the buckling strength and buckled shape of the compression web member of interest, an alternative method was developed. Section 3.1.1 discusses the steps that were taken in an effort to develop an

equivalent model of this compression web member and thereby perform accurate buckling analyses.

3.1.1 Methodology

The equivalent column method was developed to produce an independent model of the web member of interest. In this method the resistance provided by the top and bottom chords and the adjacent web members within the original truss are represented by rotational and translational springs. This method was based on a theoretical approach to column buckling outlined in the *Guide to Design Criteria for Metal Compression Members (*Johnston, 1966).

The *Guide to Design Criteria for Metal Compression Members* outlines an approach to assist in the analysis of centrally loaded compression members where the rotational and translational restraints are known. Once these values are determined, a model of the column can be made representing these restraints as rotational and translational springs, (Figure 3.5).

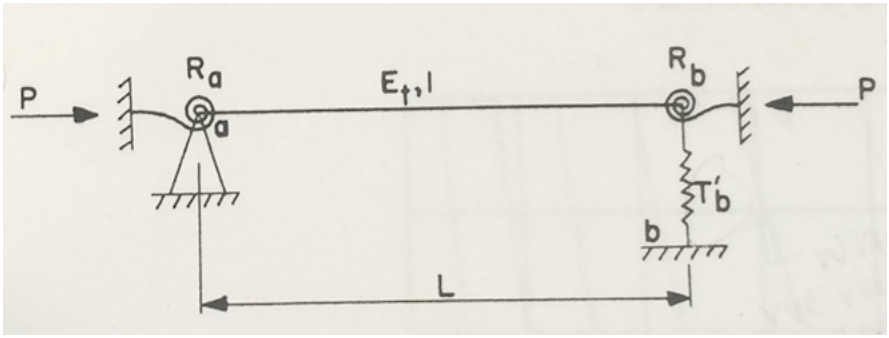

Figure 3.5. Rotational and Translational End Restraint modeled with springs (Johnston, 1966)

In this diagram, the rotational end restraints at both ends are known values, R_a and R_b, and the translational restraint, which is also known, can be replaced by an equivalent restraint at one end. In order to determine the rotational and translational spring values corresponding to the truss system being studied, the procedure outline in the next section was followed. The subsequent sections detail the process developed in order to determine the rotational and translational stiffness provided by the chords and tension web members that frame into the top and bottom connections.

3.1.1.1 Rotational Restraint from Top Chord

In order to create an accurate equivalent model, it was necessary to isolate the resistance provided by the top and bottom chords separately. To determine the resistance provided solely by the top chord and tension web members that frame into the top connection, the bottom connection of the web member of interest was completely fixed, see Figure 3.6. The member of interest was then buckled using the self-equilibrating induced-compression (SEIC method, Appendix E). SEIC is a targeted analysis method developed

by Lee (2013) as a means for controlling when a particular member will buckle within an entire truss system.

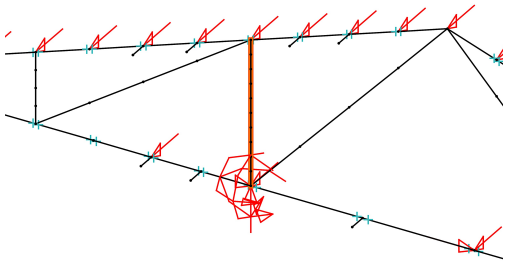

Figure 3.6. MASTAN2 Model with bottom chord connection fixed

Once a buckled shape and load for the compression member of interest were determined, a separate model isolating solely the member of interest was made as shown in Figure 3.7 (a). The bottom connection was modeled as fixed and the top connection was modeled with an in-plane translational fixity and a rotational spring to represent the rotational resistance provided by the top chord. The translational fixity was necessary due to the frequency of out-of-plane bracing along the top chord of the truss; in which it assumed that out-of-plane movement is restrained at all joints. To model these end conditions within MASTAN2, as shown in Figure 3.7 (b), the necessary fixities were applied. The model material and section properties matched those from the full truss model. The fixed connection at the bottom was modeled by restraining translation and rotation in all degrees-of-freedom. To model the rotational spring at the top, the in-plane rotation was completely fixed and the flexural connection stiffness value was varied to adjust the value of the rotational spring constant, k_r.

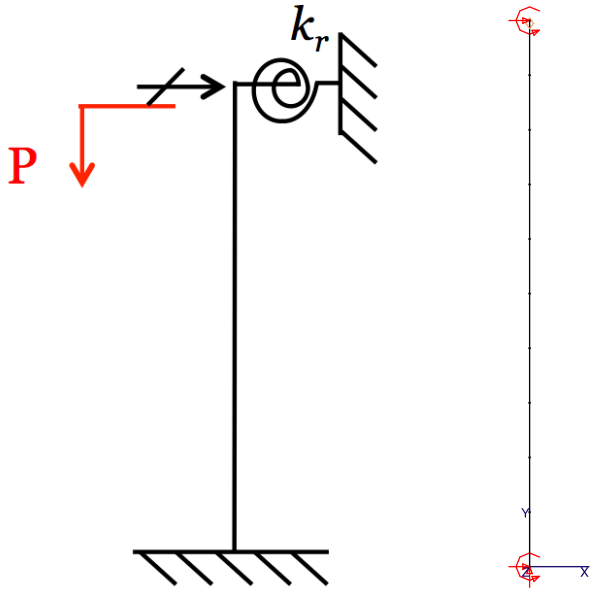

(a) Theoretical diagram (b) MASTAN2 model

Figure 3.7 (a) & (b). Isolated member of interest to determine top chord restraint

An elastic critical load (buckling) analysis was then performed on this model, using the SEIC method. This analysis was repeated while varying the stiffness of the rotational spring, k_r, until the buckling load of the equivalent model matched those generated from the full truss analysis. The derived value of the rotational spring thereby represents the rotational restraint provided by the top chord of the truss.

3.1.1.2 Rotational Restraint from Bottom Chord

To determine the resistance provided by the bottom chord, the same method was applied by initially fixing the top chord connection (Figure 3.8). Due to the decreased spacing of out-of-plane bracing along the bottom chord of the truss, the isolated model

representative of the resistance provided by the bottom chord must incorporate both rotational and translational springs (Figure 3.9).

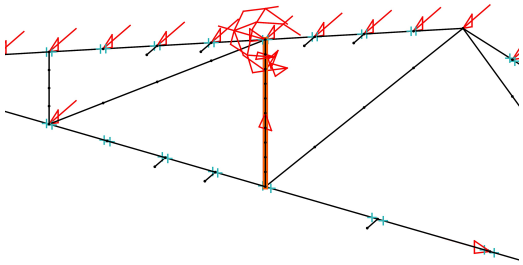

Figure 3.8. MASTAN2 Model with top chord connection fixed

In order to determine the appropriate combination of the translational spring stiffness, k_t, and rotational spring stiffness, k_r, which would produce the same buckled shape as that from the full truss system analysis, combinations of k_t+k_r had to investigated. To do so, SEIC analysis was applied while systematically varying the rotational and translational spring values, until an accurate combination as determined that match the buckling load from the truss analysis.

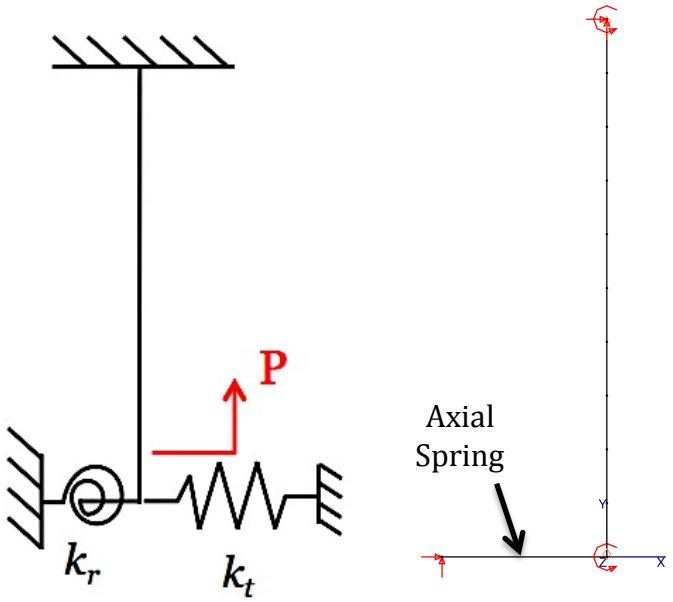

(a) Theoretical diagram (b) MASTAN2 model

Figure 3.9 (a) & (b). Isolated member of interest to determine bottom chord restraint

3.1.1.3 Equivalent Column Investigation

Once the rotational and translational stiffness provided by the top and bottom chords was determined through the previously outlined method, a combined equivalent system was created as shown in Figure 10. The resulting equivalent system models the combined translational and rotational restraint acting on the compression web member of interest, provided by the top and bottom chords, and adjacent tension members. This configuration now mirrors the system shown in Figure 3.5. The development of this model made it possible to run buckling analyses and determine the buckling strength of the compression web member without running analyses of the full truss.

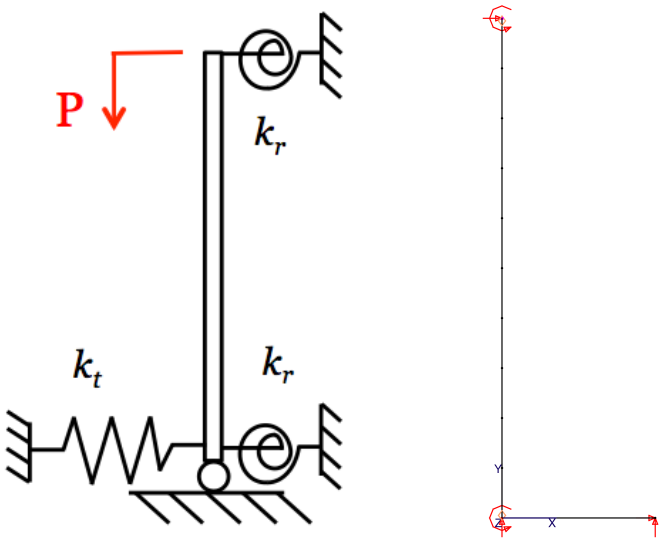

(a) Theoretical diagram (b) MASTAN2 model

Figure 3.10 (a) & (b). Equivalent system representative of compressive web member

3.1.2 Results

3.1.2.1 Introduction to Computer Analysis Results

The primary focus of the computational section of this thesis was on the complete analysis of a cold-formed steel roof truss, which is a Pratt truss without a central vertical member. In order to focus the buckling failure mode on the compression web member of interest to this study, the SEIC method, was used in the full truss analysis in conjunction with individual analyses of equivalent models. The collected results explore the additional stiffness effects provided by the chords and tension members while varying the

connection stiffness from pinned (no flexural restraint provided by connections) to completely rigid connections.

3.1.2.2 Equivalent Column Model

The equivalent column method, as detailed in Section 3.1.1, was developed as a means of isolating and studying the compression web member of interest. This was accomplished by developing a model that uses rotational and translational springs to simulate the flexural and torsional stiffness provided by the top and bottom chords and adjacent tension members. The results provided in this section were derived using the method in Section 3.1.1; the complete numerical results are shown in Appendix F.

3.1.2.2.1 All Rigid Connections

The results presented in Table 3.1 are obtained by applying the equivalent column method on the modified Pratt truss system, assuming rigid connections throughout the entire truss excluding the end connections of the web member of interest.

Table 3.1. Results from Equivalent Column Method Assuming Rigid Connections

Translational Spring Stiffness, k_t (k/in) *without initial k_t	**P_{cr} (k)**	***K* –factor web**	**Translational Spring Stiffness, k_t (k/in) *with initial k_t=0.18**	**P_{cr} (k)**	***K*-factor web**
0	3.3	1.16	0.18	8.4	0.72
0.0125	3.6	1.10	0.2	9.0	0.70
0.075	5.4	0.90	1	13.2	0.58
0.5	13.2	0.58	1000	13.2	0.58

3.1.2.2.2 All Pinned Connections

Table 3.2 presents similar results but now assuming all web members except the compression member of interest had pin connections at both ends.

Table 3.2. Results from Equivalent Column Method Assuming Pinned Connections

Translational Spring Stiffness, k_t (k/in) *without initial k_t	**P_{cr} (k)**	***K* –factor web**	**Translational Spring Stiffness, k_t (k/in) *with initial k_t=0.07**	**P_{cr} (k)**	***K*-factor web**
0	3.1	1.19	0.07	5.1	0.92
0.005	3.2	1.17	0.5	9.0	0.70
0.05	4.6	0.98	1	12.6	0.59
0.5	12.6	0.59	1000	12.6	0.59

3.2. Full Truss Analysis

An additional computational study was performed on the full truss system employing the SEIC method in order to observe the behavior of the entire system when the compression web member of interest is intentionally buckled within the full system.

3.2.1 Methodology

Two models were analyzed in order to account for any variation in the connections within the truss. The first model was identical to the truss system shown in Figure 3.2, where all end connections were rigid, while the second model had all pinned end connections, with

the exception of the member of interest. Both of these models were analyzed through the application of SEIC, and running elastic critical load (buckling) analyses in MASTAN2.

3.2.2 Results

In order to induce failure of the intended web member, the SEIC method was applied within a full truss model. Table 3.3 provides a summary of the critical buckling loads found through application of SEIC and the corresponding back-calculated critical buckling length *K*-factors.

Table 3.3. Results from SEIC Analysis of Full Truss

	Critical Buckling Load, P_{cr} (k)	*K*-Factor
All Rigid Connections	10.8	0.64
Web Members Pinned at Both Ends*	5.8	0.87

* Member of interest not pinned at both ends

3.3 Limitations

The results presented in this section have several associated limitations. First, in order to model the modified Pratt truss from the provided specifications in MASTAN2, assumptions were made concerning the connection and dimensioning details that were not clearly provided by the manufacturer. This connection uncertainty was addressed in this chapter through the repetition of the computational truss studies assuming both fully rigid and fully pinned connections throughout the entire truss system.

The applicability of the collected results to other full-scale truss systems is not entirely clear because most of the methodology employed was specific to this particular study. While the method is supported by known theory, continued research is necessary to validate the accuracy of the equivalent column method and associated results.

CHAPTER 4: SUMMARY OF RESULTS

4.1 Summary of Experimental Results (Inverted King Post Truss)

The results of the experimental testing provide an opportunity to physically examine the tensioning effects of web and chord members on the buckling strength (and associated effective length factors) of compression web members. Based on the governing differential equations, it was expected that the effective length factor corresponding to the roller support would be $K = 2.0$ and the K-factor resulting from the cable model would be 1.0. This mathematical study supported the theory presented in Lee's thesis, and clearly showed that the resisting force (developed in the model with added tension members) tracks a chord defined by the member ends, thereby providing an upper limit for the K-factor at a value of 1.0. The experimental results, in addition to computational studies modeling the apparatus geometry, corroborate this theory.

Through additional computational analysis of the experimental systems, various factors were explored to determine the potential variability of the resulting critical buckling loads and associated effective length factors. The computational study exploring the effects of varying rotational stiffness provided by connections showed that the roller system was highly sensitive to any reduction in rotational stiffness, resulting in the critical buckling load dropping significantly when a slight reduction in stiffness occurred. Conversely, the model with added tension cables was not impacted by any reduction in rotational stiffness. In fact, as soon as the bottom member-to-cable connection developed any rotational restraint, the effective length factor decreased below 1.0, and reached a value

as low as 0.5 for a fully rotationally restrained condition at both ends.

4.2 Summary of Computational Results (Modified Pratt Truss)

The computational studies performed on the modified Pratt truss provided an alternative method to investigate the out-of-plane resistance of compression members provided by tension web and chord members. The SEIC bucking analysis of the compression web member of interest within a full truss system produced effective buckling length factors ranging from 0.64 to 0.87, which are dependent on the connection rigidity within the truss. This suggests that the rotational resistance provided by the entire system could be sufficient to warrant the use of *K*-factors less than 1.0.

The equivalent column method developed through the course of this research provided a more accurate model of the rotational and translational restraint provided by the top and bottom chords. This restraint was modeled by use of rotational and translational springs on an isolated model of the compression web member of interest. The results of this study show that a *K*-factor of 1.16 to 1.19 (depending on the degree of connection rigidity in the truss) will only occur when there is no out-of-plane translational resistance provided by the bottom chord. However, the presence of any out-of-plane bracing or the tension effect of a bottom chord, which is standard in truss design, will provide translational restraint and thereby reduce the effective length factor of the web members. The results of this study suggest that values as low as 0.59 to 0.72 could be considered for use in design.

CHAPTER 5: CONCLUSIONS

5.1 Conclusions

For compression web members in trusses, the top and bottom chords provide the only acknowledged flexural and torsional resistance. Previous research performed on open-web steel joists suggests that adjacent tension web members may provide additional out-of-plane flexural stiffness that could be accounted for in the calculation the effective length factors (Lee and Ziemian, 2014). Lee's research suggests that the rotational restraint resulting from the tracking behavior of the resisting force, which is developed by the existence of neighboring tension members, could ensure that the *K*-factor would not need to exceed a value of 1.0. Through the development of an experimental testing apparatus, this study confirmed the tracking behavior of the tension cable model. By varying the physical parameters through computational analysis, this study confirmed that regardless of the degree of rotational restraint provided by the end connections of a member surrounded by tension members, a *K*-factor of 1.0 would not be exceeded. The exploration of the tensioning effect on compression web members leads to a greater understanding that neighboring tension members have an impact on the out-of-plane buckled strength of compression members. It supports that such influence should be further explored and accounted for in design guides.

Previous studies have been primarily limited to computer analysis of truss or joist systems, focusing on in-plane buckling behavior of compression web members. The

experimental testing portion of this study provides a unique opportunity to observe the interaction between tension and compression web members within a smaller system. In particular, the effect that tension members have on the direction of the resisting force that develops during buckling, which appeared to prevent *K*-factors from exceeding 1.0. The computational studies presented within this thesis suggest that the rotational restraint provided to a compression web member through interaction with tension members in an entire truss system is substantial and a *K*-factor of less than 1.0 could be used in design.

5.2 Recommendations for Future Work

The results of this study are limited as discussed in Sections 2.1.3 and 3.3. The limitations are a result of the experimental nature of the research along with the limited focus on one computational model. As a result of these limitations, additional research related to this study is necessary in order to conclusively state that a *K*-factor of less than 1.0 is appropriate for use in compression web member design. Two potential areas for future work include (i) larger-scale experimental testing of steel truss systems and (ii) computational studies performed on a variety of truss types.

The limitations associated with small-scale testing were addressed in Section 2.1.3 in order to confirm that the results found in this research apply to full-scale systems. As a result, additional experimental research should be conducted on steel systems to accurately determine how steel systems behave.

Additional computational studies of various truss configuration should be performed and analyzed with a variation of loading conditions to ensure that trusses subject to a variety of loading cases experience the same effects as those observed in this study.

BIBLIOGRAPHY

AISC (2010). *ANSI/AISC 360-10 Specification for structural steel buildings*. (14th ed.). Chicago, Ill.: American Institute of Steel Construction.

ASTM Standard D790, 2002, "Standard Test Methods for Flexural Properties of Unreinforced and Reinforced Plastics and Electrical Insulating Materials," ASTM International, West Conshohocken, PA, 2002, DOI: 10.1520/D790-02,www.astm.org.

Johnston, B. G. (1966). *Guide to design criteria for metal compression members* (2nd Edition ed.) John Wiley & Sons Inc.

Lee, S. (2013). Effective length K-factors for flexural buckling strengths of web members in open web steel joists. (Master of Science in Civil Engineering, Bucknell University).

Lee, S. G., & Ziemian, R. D. (2014). Effective length K-factors for flexural buckling strengths of web members in open web steel joists. *Proceedings of the Annual Stability Conference,* Toronto, Canada. pp. 452.

Leet, K., Uang, C., & Gilbert, A. (2010). *Fundamentals of structural analysis* (4th ed.) McGraw Hill Education.

Steel Joist Institute (2010), *Standard Specifications and Load and Weight Tables for Steel Joists and Joist Girders*, 43rd ed.

Ziemian, R.D., and McGuire, W. (2013) *MASTAN2*, <www.mastan2.com>

APPENDICES

Appendix A: Experimental system member sizing and slenderness ratio

- Check use of ¼ inch radius acrylic rod
  - Roller apparatus (K = 2.0): L = 12”

$$P_{cr} = \frac{\pi^2 EI}{(KL)^2} = \frac{\pi^2 (290{,}000\ psi)\frac{\pi}{4}(0.25)^4}{(2.0 * 12)^2} = 22.1\ lb$$

  - Cable apparatus (K = 1.0): L = 16”

$$P_{cr} = \frac{\pi^2 EI}{(KL)^2} = \frac{\pi^2 (290{,}000\ psi)\frac{\pi}{4}(0.25)^4}{(1.0 * 16)^2} = 50.7\ lb$$

*NOTE: Length difference between set-ups intended to reduce buckling load necessary for cable apparatus.

  - Check slenderness ratio: L = 16”

$$r = \sqrt{\frac{I}{A}} = \sqrt{\frac{\frac{\pi}{4}R^4}{\pi R^2}} = \sqrt{\frac{R^2}{4}} = \frac{R}{2} = \frac{0.25}{2} = 0.125$$

$$\frac{L}{r} = \frac{16}{0.125} = 128 > 100$$

  - Check slenderness ratio: L = 12”

$$r = \sqrt{\frac{I}{A}} = \sqrt{\frac{\frac{\pi}{4}R^4}{\pi R^2}} = \sqrt{\frac{R^2}{4}} = \frac{R}{2} = \frac{0.25}{2} = 0.125$$

$$\frac{L}{r} = \frac{12}{0.125} = 96 \cong 100$$

Appendix B: Schematic of Experimental Testing Apparatus

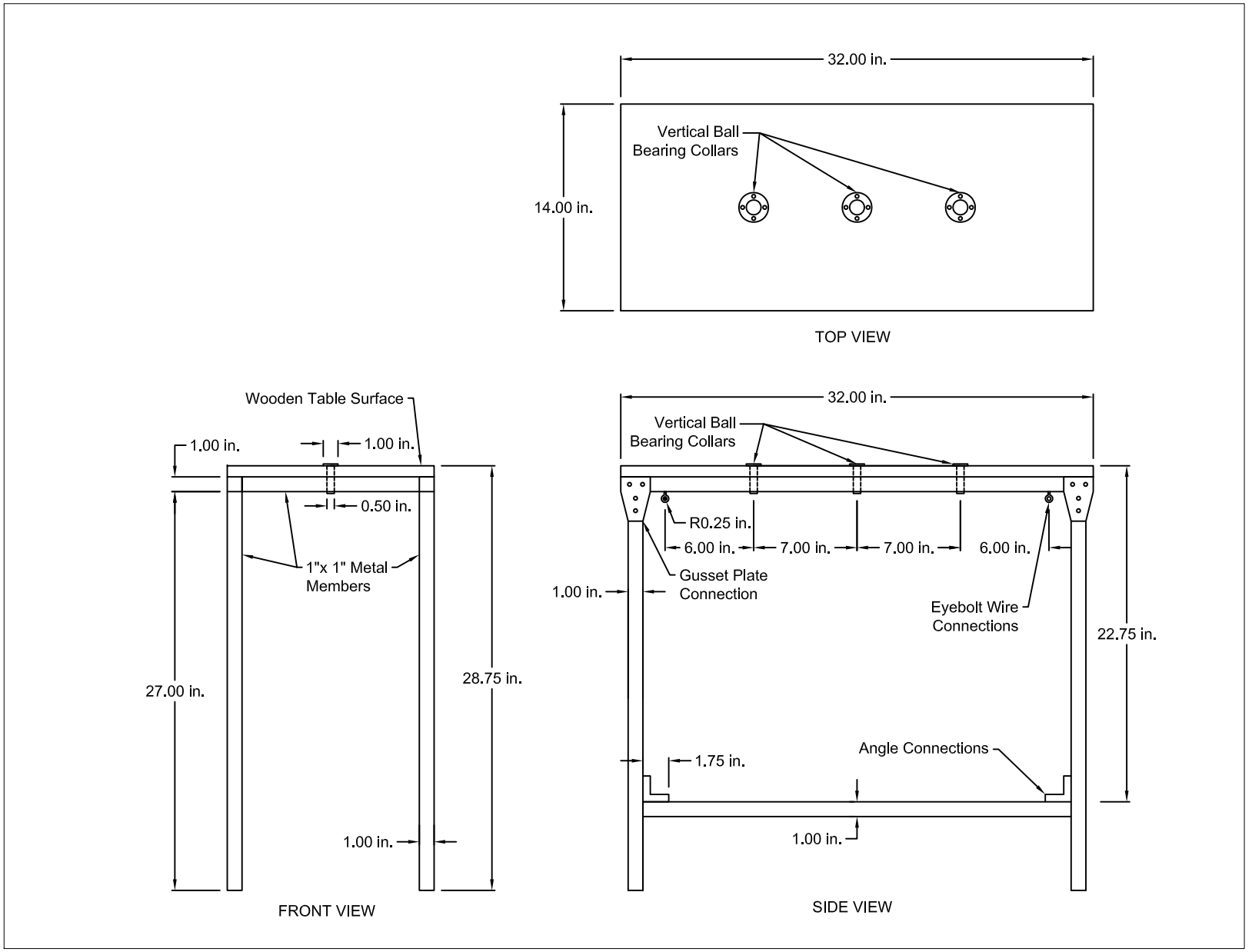
32.00 in.
Vertical Ball
Bearing Collars
14.00 in.
TOP VIEW
Wooden Table Surface
1.00 in.
1.00 in.
0.50 in.
1"x 1" Metal
Members
27.00 in.
28.75 in.
1.00 in.
FRONT VIEW
32.00 in.
Vertical Ball
Bearing Collars
R0.25 in.
6.00 in.
7.00 in.
7.00 in.
6.00 in.
1.00 in.
Gusset Plate
Connection
Eyebolt Wire
Connections
22.75 in.
Angle Connections
1.75 in.
1.00 in.
SIDE VIEW

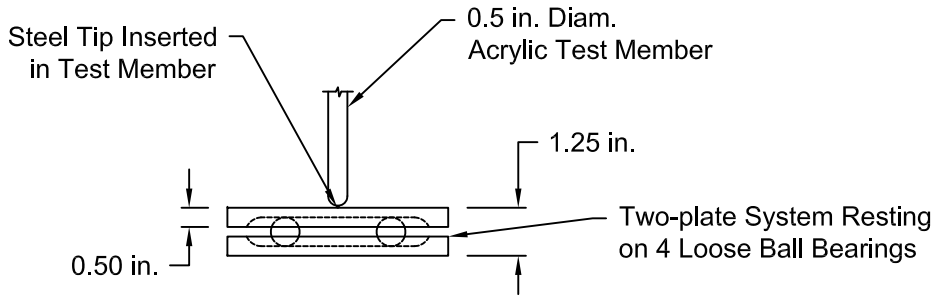

Front View of
Roller System

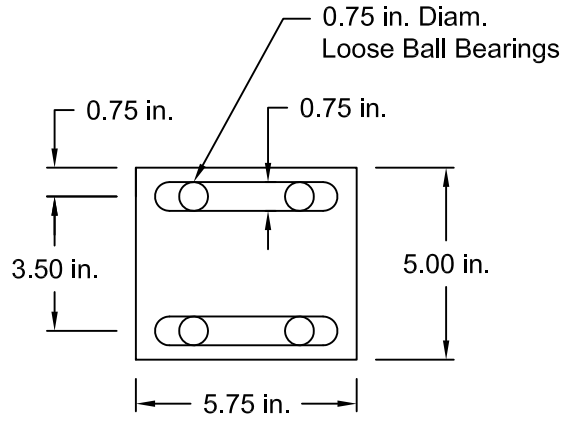

Top View of One Plate
w/ Loose Ball Bearings

Appendix C: Cross Section properties of modified Pratt truss

Member Designation	Wt. (lbs/ft)	Area (in^2)	I_x (in^4)	I_y (in^4)	J x 1000 (in^4)
Bottom Chord 25USC 035 50	0.68	0.200	0.184	0.038	0.090
Top Chord 35USC 035 50	1.01	0.296	0.477	0.079	0.134
Webs 15USW 035 50	0.45	0.132	0.049	0.016	0.060

All members: Modulus of elasticity, *E*, was assumed to be 29,500 ksi

Appendix D: SEIC Procedure (Lee, 2013)

Equivalent Column Method Steps

1. *Subdivide the compression web member of interest into 10 elements along its length*
2. *Define an element parallel to the web member of interest that has exactly the same geometric and material properties as the web member of interest.*
3. *Define connections at end of parallel element as pinned (hinges).*
4. *Apply a positive temperature load to the parallel member, thereby compressing web member of interest. No other loads, including self-weight, are to be applied to the joist.*
5. *Perform three-dimensional elastic critical load analysis of the joist system.*
6. *Observe and confirm buckling mode and load of the web member of interest.*
7. *Back-calculate effective length K-factor from buckling force in the web member of interest.*

Appendix E: Equivalent column method detailed calculations

Case 1: All connections in truss are rigid

→ *Determine rotational and translational resistance provided by bottom chord and framing tension web members:*

1. Run SEIC analysis on MASTAN2 full truss system and restrain all degrees of freedom at the top connection of compression member of interest

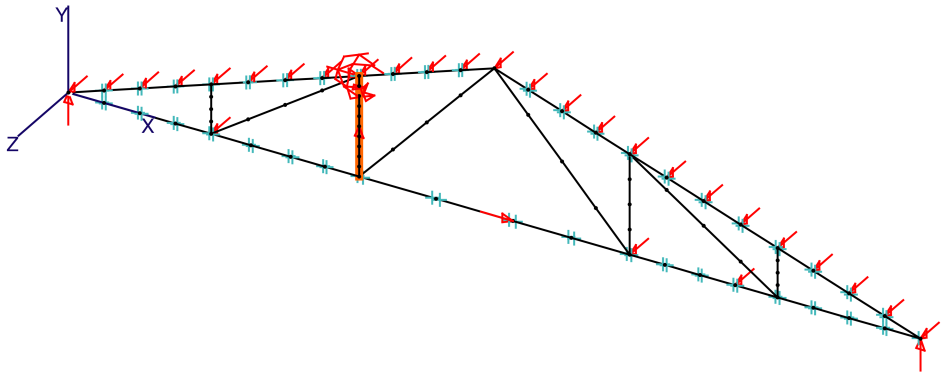

Resulting critical buckling mode: **P_{cr} = 7.39 k**

2. Back calculate *K*-factor

$$K = \frac{\pi}{L}\sqrt{\frac{EI}{P_{cr}}} = \frac{\pi}{32.564\ in}\sqrt{\frac{29500\ ksi * 0.016\ in^4}{7.39\ k}} = 0.77$$

3. Create sample column in MASTAN2 and determine rotational spring stiffness, k_r, and translational spring stiffness, k_t, that produces the same *K*- factor as previously calculated

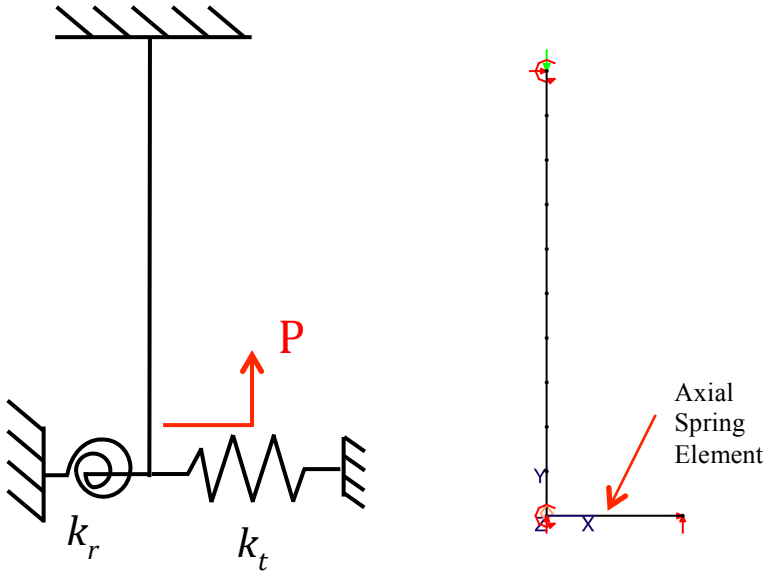

- MASTAN2 model:
  - Translational spring is modeled as an element with properties as defined below

MASTAN2 Axial Spring Element Properties

Member Property	
Area, A (in^2)	10
Length, L (in)	10
Moment of Inertia, I_x (in^2)	10
Moment of Inertia, I_y (in^2)	10
Torsional Constant, J (in^4)	10

  - Rotational springs are modeled by making the flexural connection at the end of the member *semi-rigid* and adjusting the rotational connection stiffness values accordingly
- Back-calculating rotational spring value, k_r, from MASTAN2 model of spring element

$$Spring\ stiffness\ equation: P = k\Delta$$

$$\Delta = \frac{PL}{EA}$$

$$k = \frac{EA}{L}$$

$$since\ A = 10\ in^2\ and\ L = 10\ in$$

$$k = E$$

Resulting spring values: k_t = 0.18 kip/inch and k_r= 160 k-in/rad

→ *Determine rotational resistance provided by top chord and framing tension web members:*

1. Run SEIC analysis on MASTAN2 full truss system and fully restrain top connection of compression member of interest

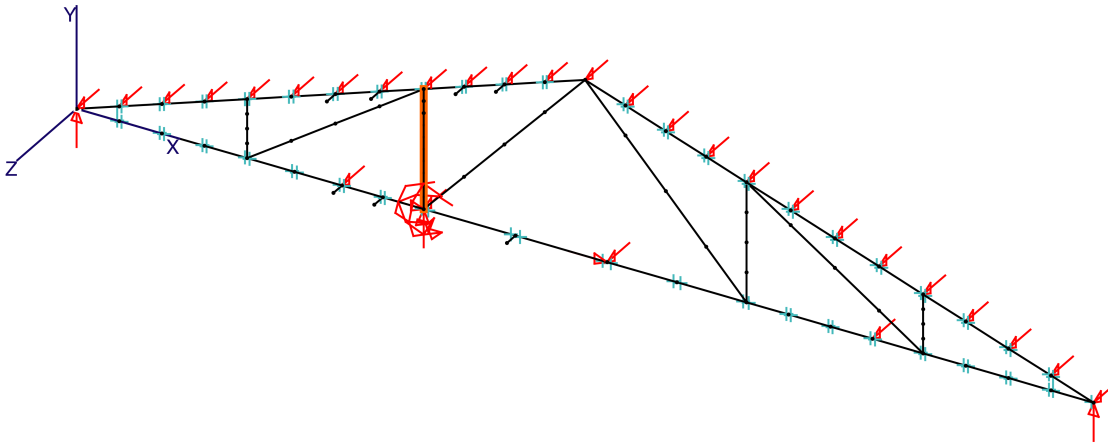

Resulting critical buckling mode: **P_{cr} = 15.17 k**

2. Back calculate *K*-factor

$$K = \frac{\pi}{L}\sqrt{\frac{EI}{P_{cr}}} = \frac{\pi}{32.564\ in}\sqrt{\frac{29500\ ksi * 0.016\ in^4}{15.17\ k}} = 0.54$$

3. Create sample column in MASTAN2 and determine rotational spring stiffness, k_r, that produces the same *K*- factor as previously calculated

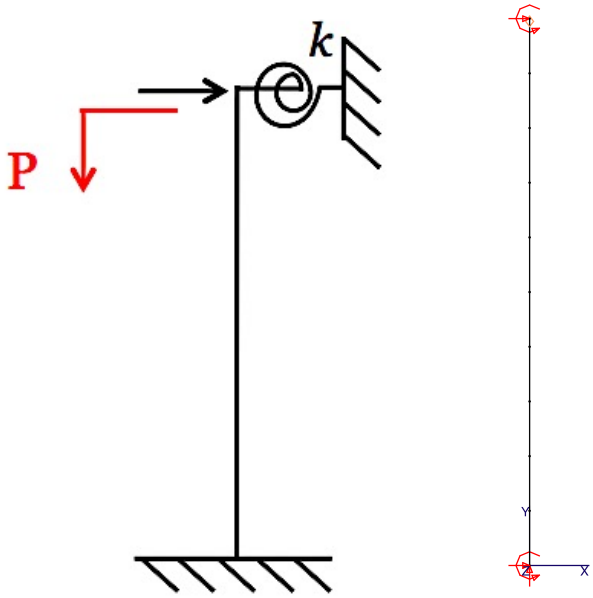

- MASTAN2 model:
  - Rotational springs are modeled by making the flexural connection at the end of the member *semi-rigid* and adjusting the rotational stiffness values accordingly
- Back-calculating rotational spring value, k_r, from MASTAN2 model of spring element

$$Spring\ stiffness\ equation: P = k\Delta$$

$$\Delta = \frac{PL}{EA}$$

$$k = \frac{EA}{L}$$

$$since\ A = 10\ in^2\ and\ L = 10\ in$$

$$k = E$$

Resulting spring values: k_r= 200 k-in/rad

→ *Produce combined equivalent column system, modeling rotational restraint provided by top and bottom chords with springs:*

1. Create sample column in MASTAN2, with combined restraint included

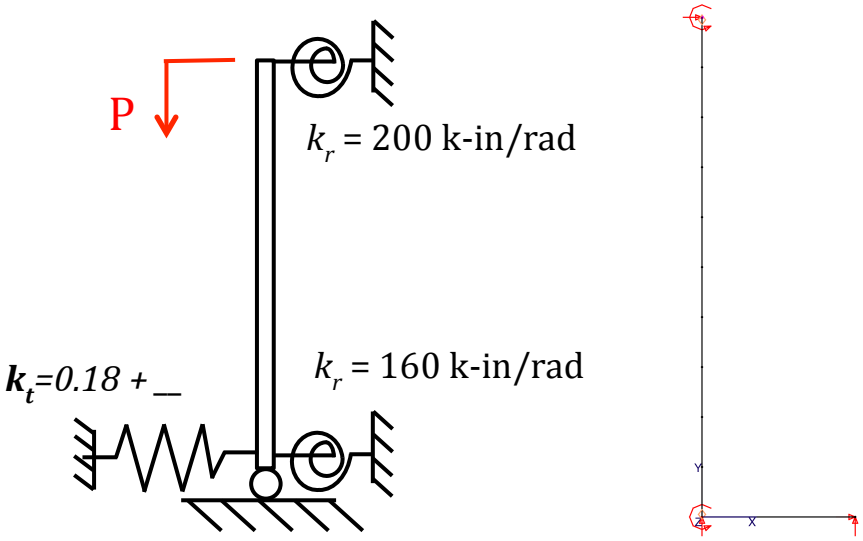

2. Determine additional translational stiffness, k_t, required to produce a *K*-factor that is less than 1.0

3. Perform SEIC analysis of the experimental system, varying translational spring stiffness values to determine stiffness required to reduce the *K*-factor of the web member to a value less than 1.0. The following results are obtained

Translational Spring Stiffness, k_t (k/in) ***without initial k_t**	**P_{cr} (k)**	***K* –factor web**	**Translational Spring Stiffness, k_t (k/in)** ***with initial k_t=0.18**	**P_{cr} (k)**	***K*-factor web**
0	3.3	1.16	0.18	8.4	0.72
0.0125	3.6	1.10	0.2	9.0	0.70
0.075	5.4	0.90	1	13.2	0.58
0.5	13.2	0.58	1000	13.2	0.58

Case 2: All connections are pinned except both ends of member of interest

→ *Determine rotational and translational resistance provided by bottom chord and framing tension web members:*

1. Run SEIC analysis on MASTAN2 full truss system and restrain all degrees of freedom at the top connection of the compression member of interest

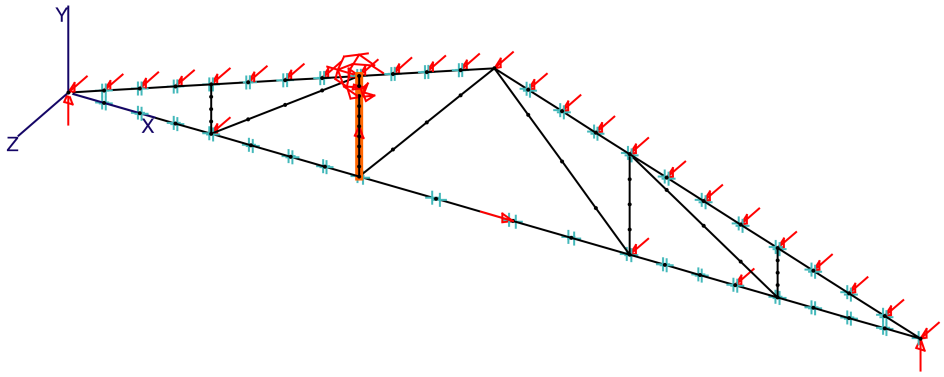

Resulting critical buckling mode: $\mathbf{P_{cr} = 5.63\ k}$

2. Back calculate *K*-factor

$$K = \frac{\pi}{L}\sqrt{\frac{EI}{P_{cr}}} = \frac{\pi}{32.564\ in}\sqrt{\frac{29500\ ksi * 0.016\ in^4}{5.63\ k}} = 0.88$$

3. Create sample column in MASTAN2 and determine rotational spring stiffness, k_r, and translational spring stiffness, k_t, that produces the same *K*- factor as previously calculated

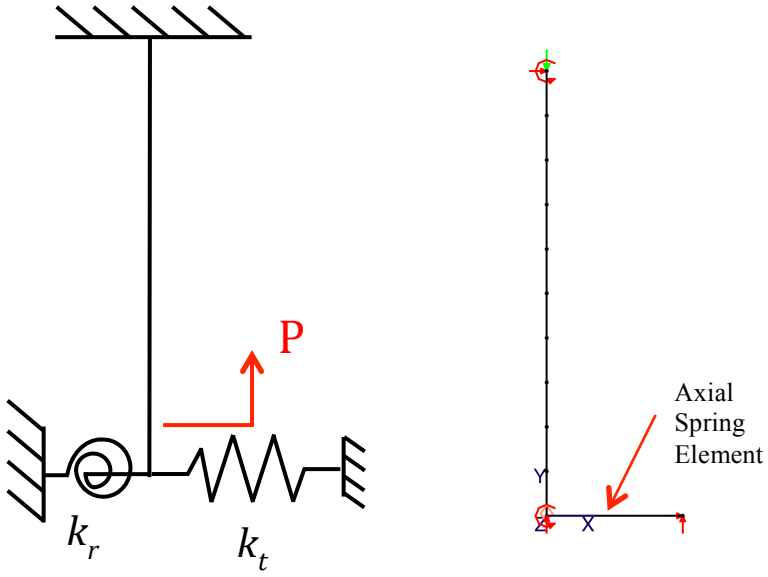

- MASTAN2 model:
  - Translational spring is modeled as an element with properties as defined below

MASTAN2 Axial Spring Element Properties

Member Property	
Area, A (in^2)	10
Length, L (in)	10
Moment of Inertia, I_x (in^2)	10
Moment of Inertia, I_y (in^2)	10
Torsional Constant, J (in^4)	10

  - Rotational springs are modeled by making the flexural connection at the end of the member *semi-rigid* and adjusting the rotational connection stiffness values accordingly
- Back-calculating rotational spring value, k_r, from MASTAN2 model of spring element

$$Spring\ stiffness\ equation: P = k\Delta$$

$$\Delta = \frac{PL}{EA}$$

$$k = \frac{EA}{L}$$

$$since\ A = 10\ in^2\ and\ L = 10\ in$$

$$k = E$$

Resulting spring values: k_t = 0.07 kip/inch and k_r= 175 k-in/rad

Determine rotational resistance provided by top chord and framing tension web members:

1. Run SEIC analysis on MASTAN2 full truss system and fully restrain top connection of compression member of interest

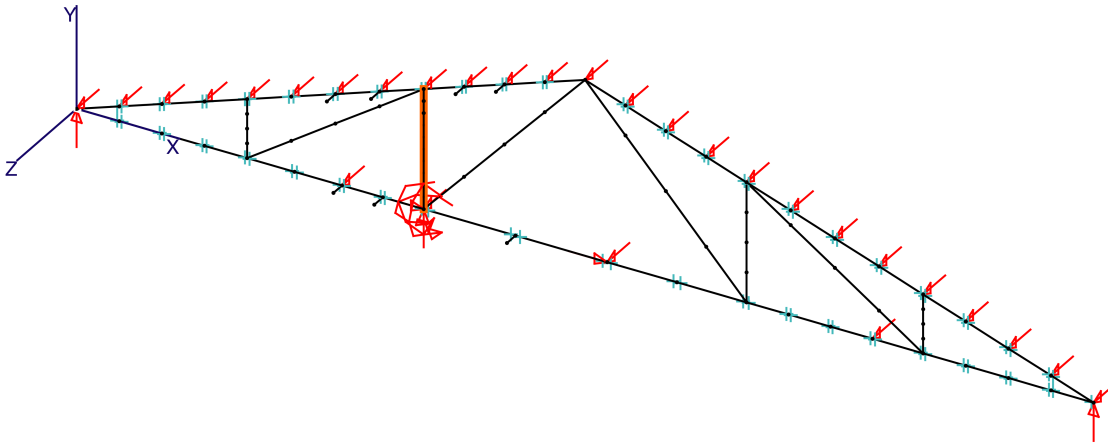

Resulting critical buckling mode: **P_{cr} = 14.66 k**

2. Back calculate *K*-factor

$$K = \frac{\pi}{L}\sqrt{\frac{EI}{P_{cr}}} = \frac{\pi}{32.564\ in}\sqrt{\frac{29500\ ksi * 0.016\ in^4}{14.66\ k}} = 0.55$$

3. Create sample column in MASTAN2 and determine rotational spring stiffness, k_r, that produces the same *K*- factor as previously calculated

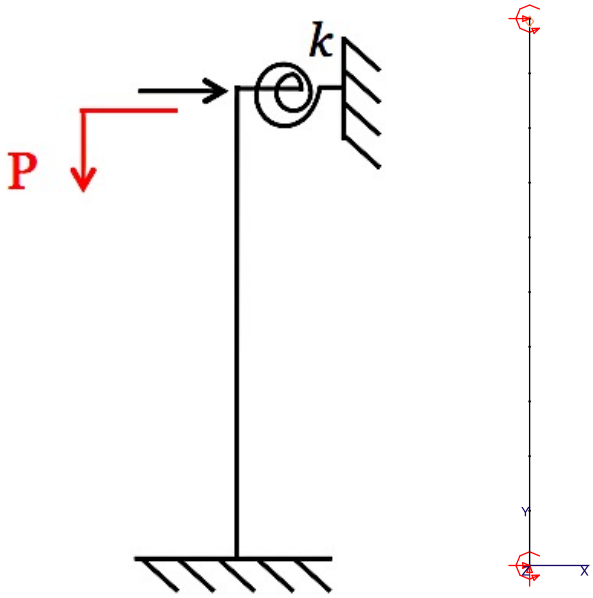

- MASTAN2 model:
  - Rotational springs are modeled by making the flexural connection at the end of the member *semi-rigid* and adjusting the rotational stiffness values accordingly
- Back-calculating rotational spring value, k_r, from MASTAN2 model of spring element

$$Spring\ stiffness\ equation: P = k\Delta$$

$$\Delta = \frac{PL}{EA}$$

$$k = \frac{EA}{L}$$

$$since\ A = 10\ in^2\ and\ L = 10\ in$$

$$k = E$$

Resulting spring values: k_r= 125 k-in/rad

→ *Produce combined equivalent column system, modeling rotational restraint provided by top and bottom chords with springs:*

1. Create sample column in MASTAN2, with combined restraint included

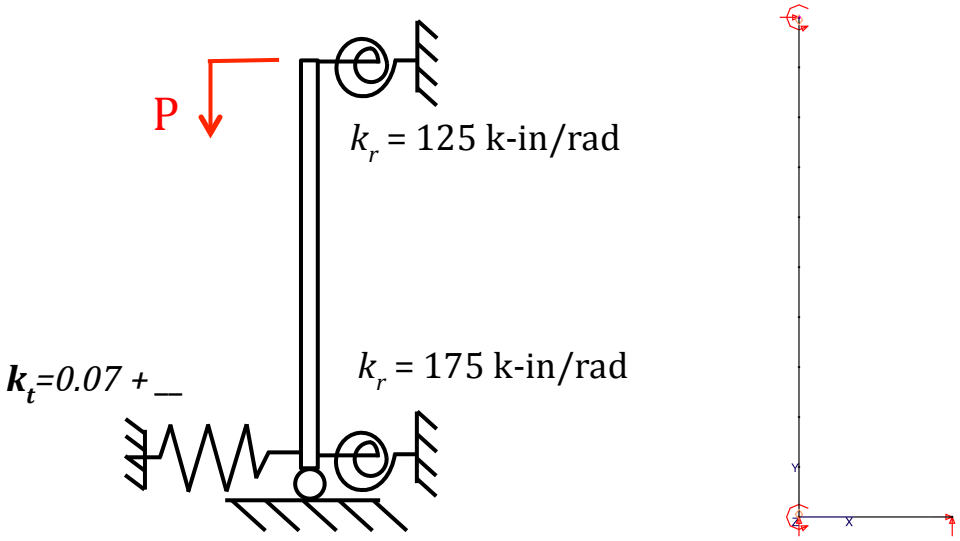

2. Determine additional translational stiffness, k_t, required to produce a *K*-factor that is less than 1.0
3. Perform SEIC analysis of the experimental system, varying translational spring stiffness values to determine stiffness required to reduce the *K*-factor of the web member to a value less than 1.0. The following results are obtained

Translational Spring Stiffness, k_t (k/in) *without initial k_t	**P_{cr} (k)**	***K* –factor web**	**Translational Spring Stiffness, k_t (k/in)** *with initial k_t=0.07	**P_{cr} (k)**	***K*-factor web**
0	3.1	1.19	0.07	5.1	0.92
0.005	3.2	1.17	0.5	9.0	12.57
0.05	4.6	0.98	1	12.6	0.59
0.5	12.6	0.59	1000	12.6	0.59